APPENDIX R

FISH LARVAE RESPONSE MODEL

Project-related impacts to Tidal Hydraulics and Potential Transport of Fish Larvae Following Terminal Groin Construction Bald Head, North Carolina

June 14, 2012
Revised September 26, 2012

Abstract. The Delft3D numerical model was employed to compute potential differences in hydraulics following construction of a semi-permeable terminal groin at the western terminus of Bald Head Island, North Carolina. The previously calibrated depth-averaged, tide-only model was reconfigured and run to describe tides during a 30-day spring-neap lunar cycle under both beach fill only and terminal groin with beach fill conditions. Several drogues were placed in the nearshore waters off Bald Head in order to track the potential hydraulic pathways of nondescript particles (hypothetical fish larvae) from the nearshore into the inlet on route to the interior estuary system. Tidal currents, drogue routes, and travel duration were directly compared under with and without project conditions. Additionally, the Delft3D particle tracking model was applied to the hydrodynamic model result in order to simulate instantaneous, localized deployment of multiple particles in the nearshore of Bald Head Island and map said particle movements and concentrations throughout the domain under with- and without- terminal groin conditions. The results of these analyses suggest that a terminal groin at Bald Head will have no far-reaching effects on the tidal hydraulics of the inlet. Differences in tidal flows are minor and localized about the general vicinity of the structure. These predicted alterations to tidal flows are not expected to meaningfully hamper the ability of suspended biota or fish larvae to reach the inlet from the nearshore waters proximate to Bald Head.

The Delft3D model was utilized to simulate the effects of the proposed terminal groin on tidal flows. Calibration of the depth-averaged model is discussed in detail under separate cover[1]. Two model domains were developed for this investigation, the first includes a 1.2 Mcy beach fill which extends along the south-facing shoreline of Bald Head between Station 166+00 and the Point. This simulation reflects erosion control measures which have been historically employed along Bald Head Island. The second model scenario includes the proposed, semi-permeable terminal groin with placement of 1.2 Mcy of beach nourishment, the distribution of which differs from the beach fill only condition in order to pre-fill the fillet east of the terminal groin requiring a beach fill which effectively terminates at about Station 130+00.

[1] Olsen, 2012. "Calibration of a Delft3D model for Bald Head Island and the Cape Fear River Entrance. Phase I." Prepared for the Village of Bald Head Island. Prepared by Olsen Associates, Inc. 2618 Herschel Street Jacksonville, FL 32204. April 2012.

The sixteen existing tube groins were conservatively represented in both models as thin dams, an impermeable and infinitely tall impediment to flow in the model. The proposed permeable terminal groin was modeled as a porous plate, the permeability of which is controlled by a friction term which was set to 4.5 for these simulations, roughly representing a level of permeability between about 10 and 30 percent by best estimation.

The tide-only model was driven by water level fluctuations derived via astronomical constituents developed by the Topex/Posiden constituent model database. Tidal phase and amplitude for the following twelve constituents were specified for 49 contiguous boundary segments along the flow domain: M2, S2, N2, K2, K1, O1, P1, Q1, MF, and MM. The model was run for a period of 30 days in order to simulate a complete spring-neap lunar cycle. Water elevation computed by the model at Southport is shown in **Figure 1**. The annual tide range shown in **Figure 2** illustrates an overall lack of significant seasonal variability in the tides near the study area, which suggests the period selected for analysis herein is a reasonable proxy for typical conditions.

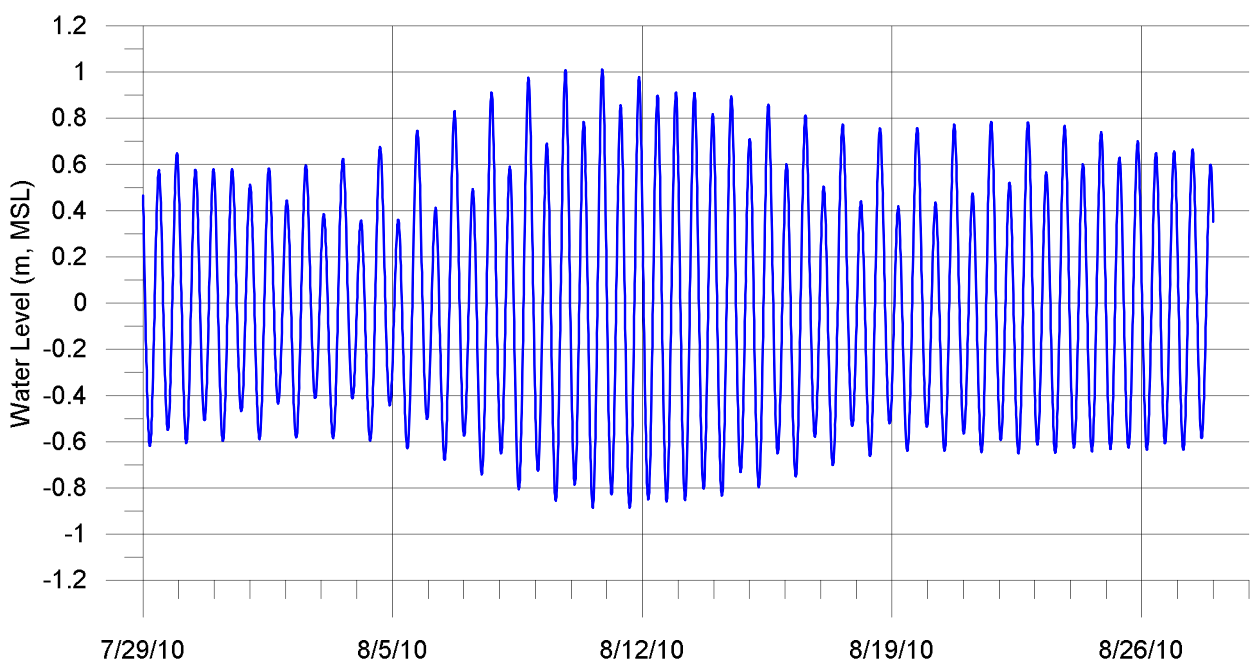

Figure 1: Computed tides at Southport for the simulation period analyzed herein.

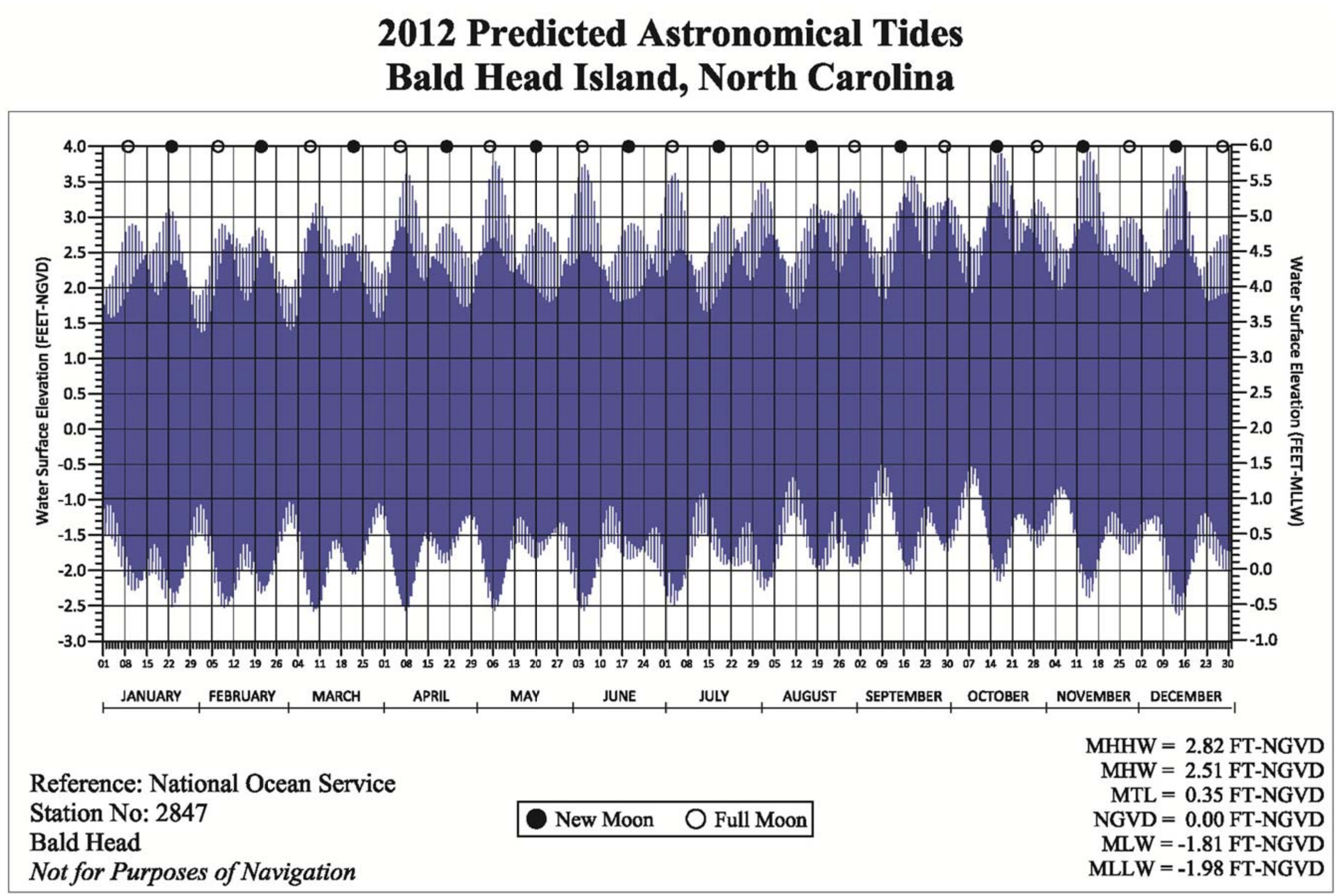

Figure 2: Predicted tides for 2012.

Figure 3 plots the residual tidal currents following the one-month simulation for the beach fill without terminal structure simulation. Residual flow is defined as the "net" flow that remains after subtracting all of the flood flow vectors from the ebb flow vectors for one lunar month. **Figure 4** comparatively plots residual flows computed under the with terminal groin condition. The model results indicate that large-scale patterns of residual flow are unchanged between alternatives. Locally, however, the terminal groin appears to accelerate ebb-directed residual flows immediately west of the structure. This is attributable to a reduction in flood tide velocity in the immediate lee/shadow of the terminal groin.

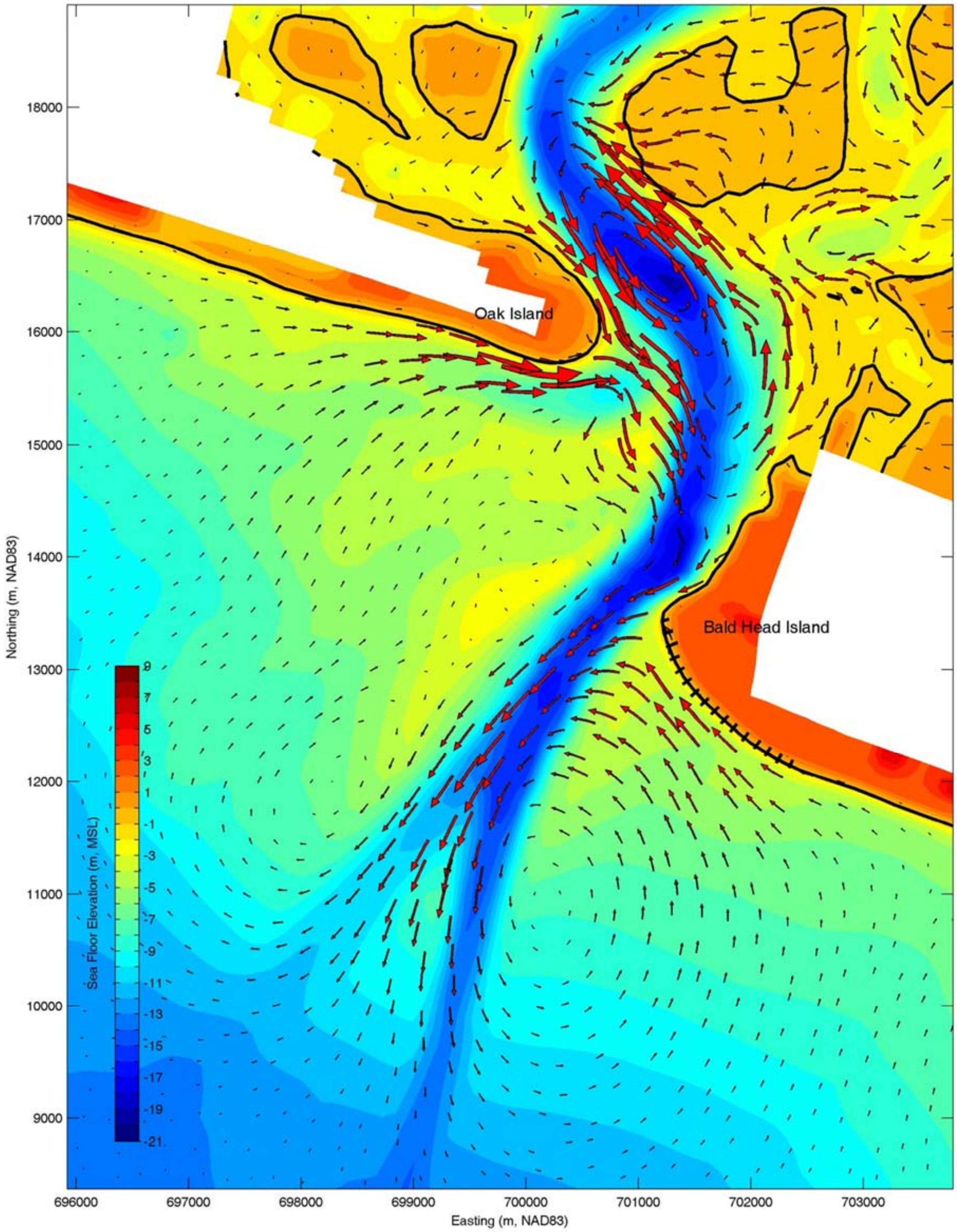

Figure 3: Residual tidal flow computed following 1-month tide only simulation under 1.2Mcy beach fill and tube groins conditions.

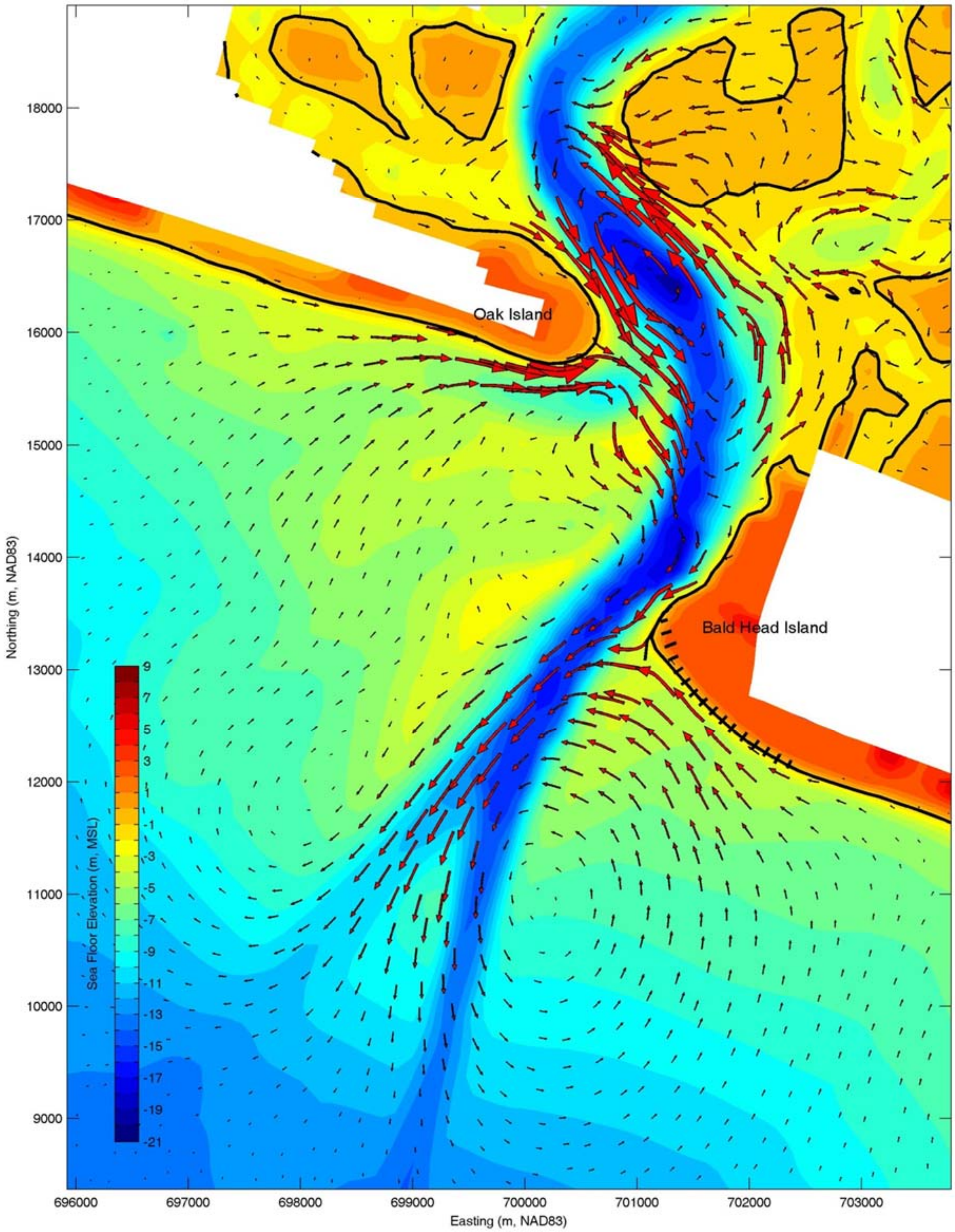

Figure 4: Residual tidal flow computed following 1-month tide only simulation under terminal groin with 1.2Mcy beach fill and tube groins conditions.

Figures 5 and **6** plot peak ebb tidal vectors and magnitudes under without- and with-terminal groin conditions, respectively. Comparison of the figures suggest the terminal groin most notably results in a modest decrease in ebb tidal velocities immediately offshore of the structure's seaward end near Bald Head Shoal. The magnitude of this decrease is on the order of 0.1 to 0.15 m/s and is limited to areas near the terminal groin. This decrease in flow velocity is partially offset by a small increase in the nearshore profile south of the groin field typically measuring less than 0.1 m/s. In terms of overall inlet hydraulics, the patterns of ebb tidal flow are not significantly altered following placement of the terminal groin.

Figures 7 and **8** plot peak flood tidal velocities and magnitudes under without- and with-terminal groin conditions, respectively. Comparison of the figures suggests that installation of the proposed terminal groin alters flood tides more significantly than the aforementioned ebb effects. This is predominantly due to (a) the reclamation of shoreline updrift and eastward of the terminal groin where with-project tides are non-existent, and (b) the redirection of flood tidal flow by the groin's seaward tip. The latter effect results in a small shadow zone in the lee of the terminal structure on a flood tide, which extends more-or-less to the limits of the navigation channel where the reduction in speed is negligible (<0.1 m/s). Peak reductions in flood tidal velocities on the order of about 0.5 m/s are identified very near the structure. The model results suggest that flood tidal velocities within, and slightly west of, the Bald Head Shoals I channel range will increase by about 0.1 m/s in response to the flow decrease computed adjacent to the proposed groin. Like the ebb tidal patterns within the inlet, the terminal structure is not predicted to have far-reaching effects on the tidal hydraulics of the inlet.

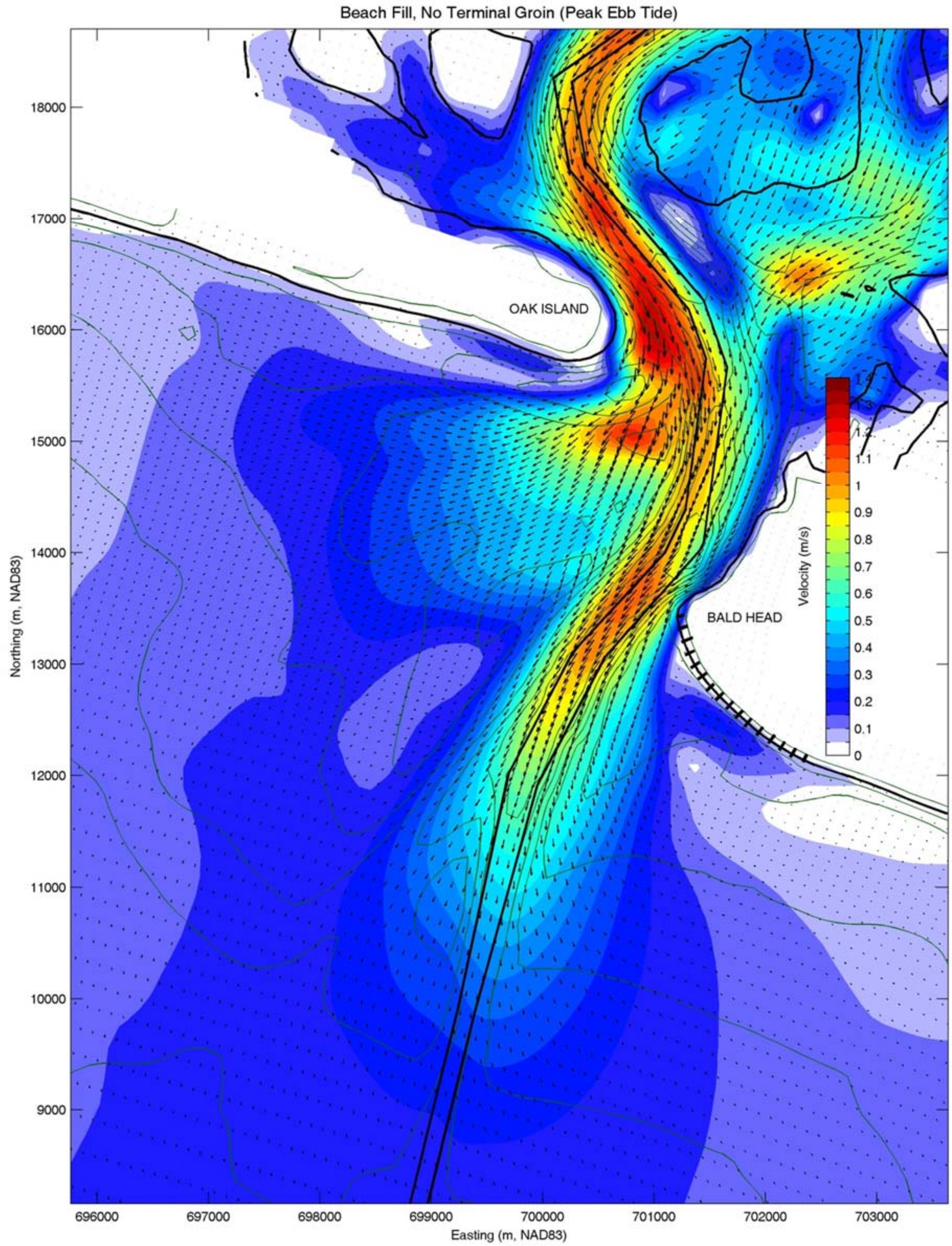

Figure 5: Peak ebb tidal flow computed following 1-month tide only simulation under 1.2Mcy beach fill and tube groins conditions.

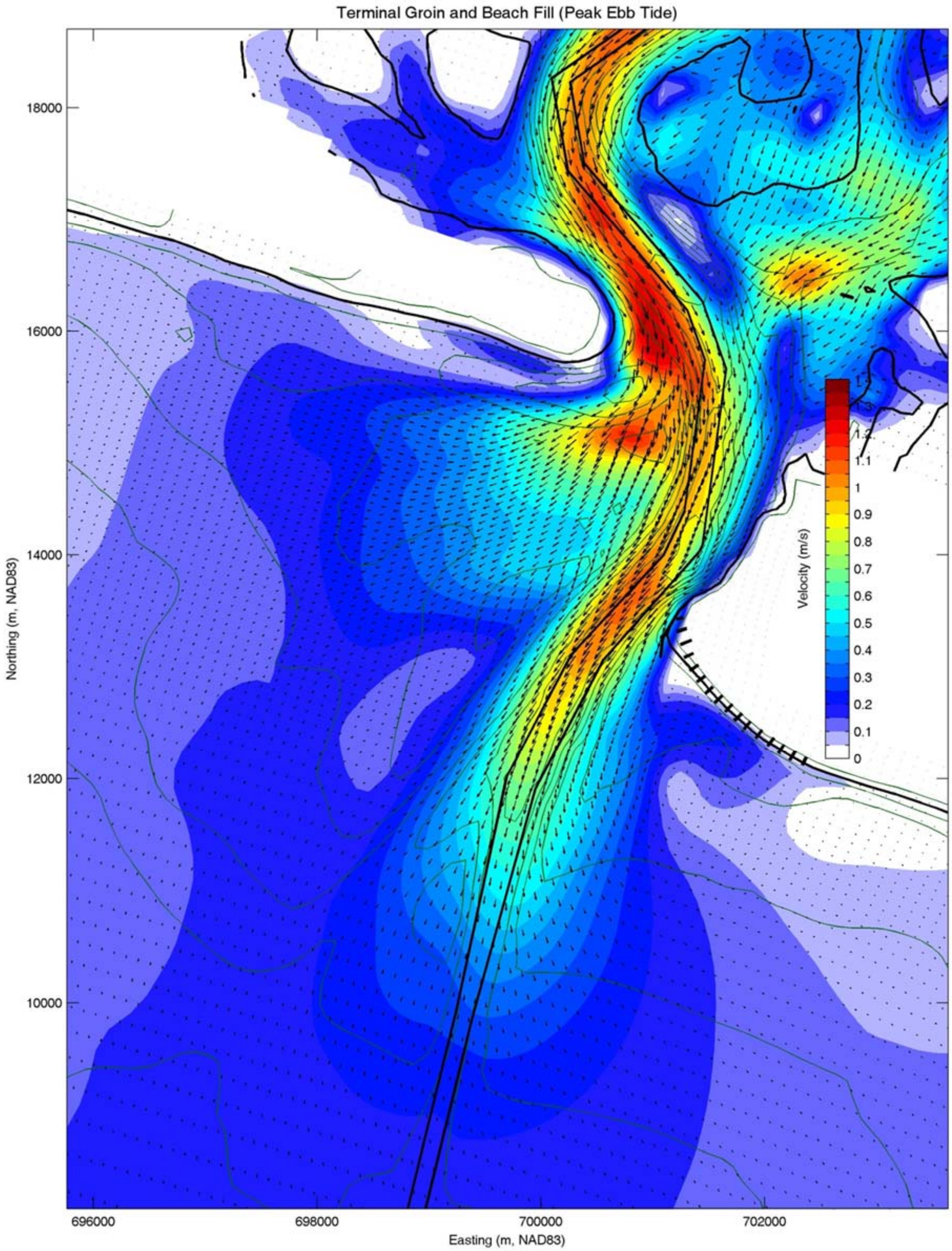

Figure 6: Peak ebb tidal flow computed following 1-month tide only simulation under terminal groin with 1.2Mcy beach fill and tube groins conditions.

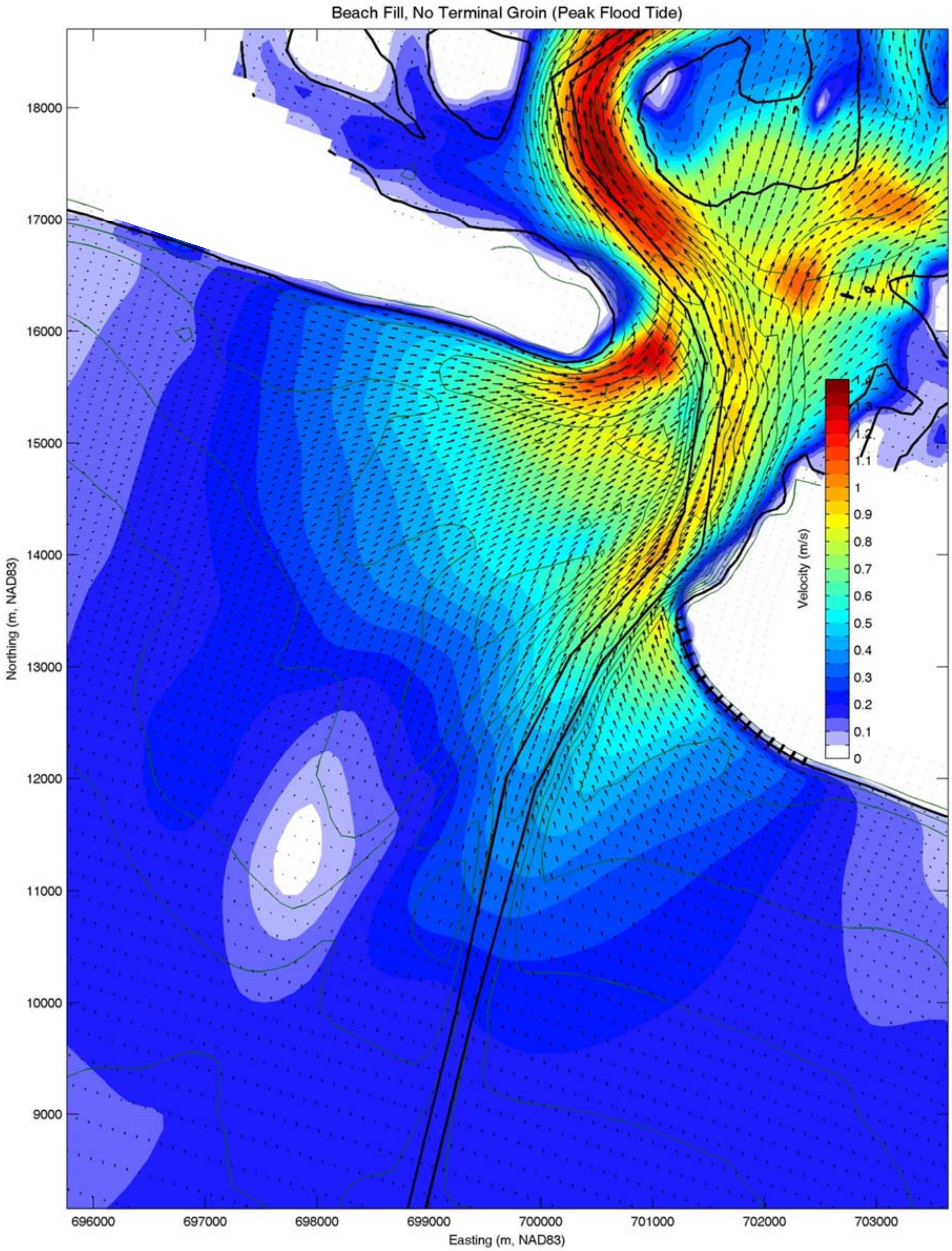

Figure 7: Peak flood tidal flow computed following 1-month tide only simulation under 1.2Mcy beach fill and tube groins conditions.

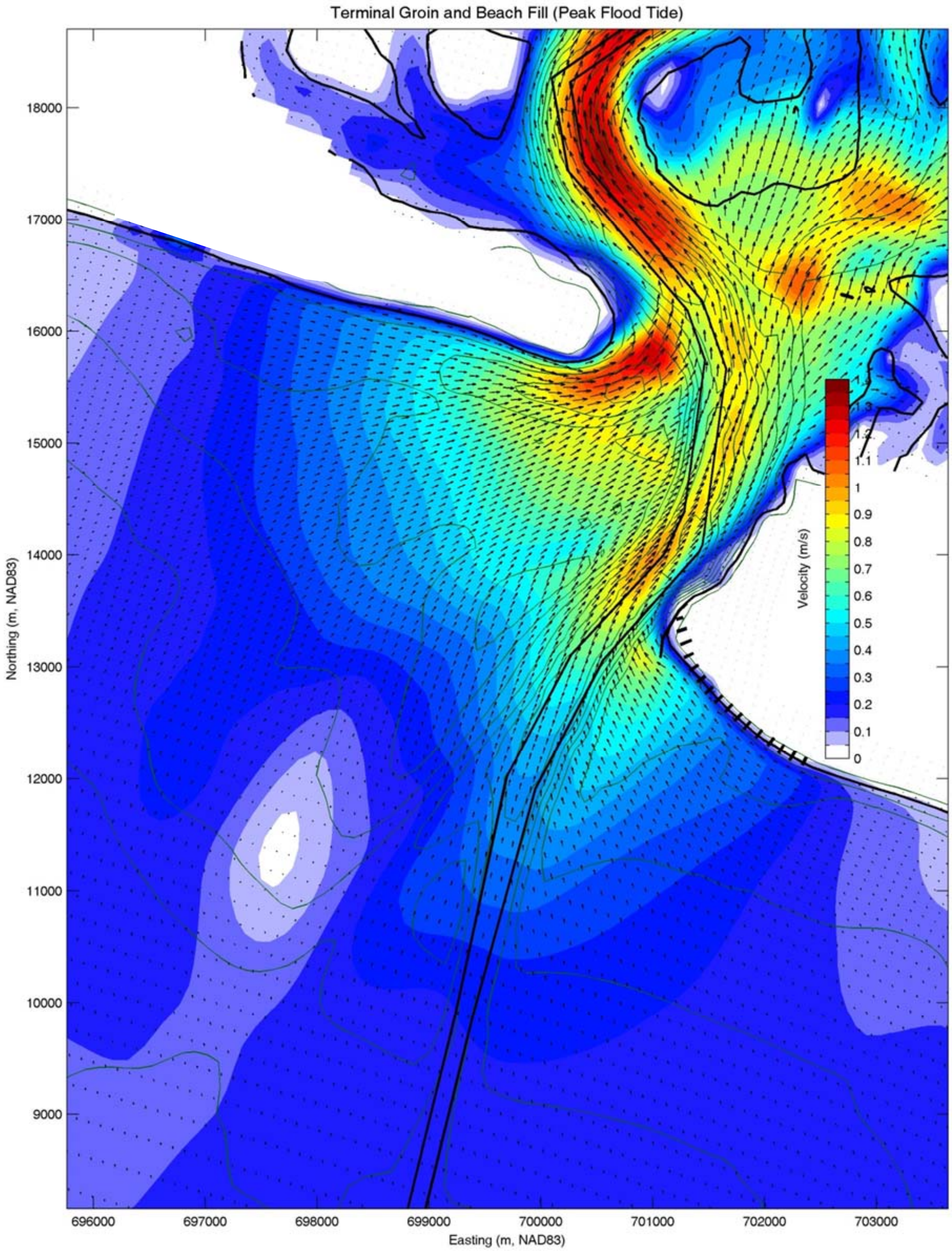

Figure 8: Peak flood tidal flow computed following 1-month tide only simulation under terminal groin with 1.2Mcy beach fill and tube groins conditions.

The hydrodynamic models were also utilized to evaluate potential changes in flow patterns which might affect the tidal transport of fish larvae from the Bald Head Island nearshore area to the inlet. Hypothetical larvae were simulated by deploying drogues at various nearshore and offshore locations within the model domain. Drogues were initially deployed at seven locations varying in distance from the inlet, see **Figure 9**. Drogue C was deployed the farthest from the inlet (about 2.1 miles east of the inlet) and is located in the nearshore in an area where flood tidal currents are respectively weak. Based on the model results shown in **Figure 7**, drogue C is located along the edge of influence the flood tidal influence where peak velocities are predicted to be less than 0.2 m/s. Drogues D through G were initially placed along a shore perpendicular azimuth beginning east of the groin field and extending slightly more than 1,500 meters offshore.

At each location, the drogues were deployed twice during the 30-day simulation. The first deployment occurred at time step one in the model which corresponds to a neap tide condition – this time step equates to 29 July 2010 00:00 in **Figure 1**. Following deployment, these drogues were tracked throughout the entire model simulation. Additional drogues were deployed at each location and tracked beginning at a time step equivalent to 17:50 hours on 10 August 2010. This time step reflects conditions present during the simulated spring tide range. The locations of drogue deployments were identical between neap and spring simulations, and deployments were timed to roughly correspond with a mid-tide. In addition to the water level data presented in **Figure 1**, water levels during the deployment are indicated on each result illustration presented below.

The path and duration of travel for each drogue was calculated and compared both with and without the terminal groin. It is assumed that once a particle passes west of the western tip of Bald Head Island and enters the inlet, it enters a hydraulic regime which is dominated by river flows, tidal currents, and pressure fields which operate well outside of the influence of the terminal groin as noted in the above discussion. **Figure 10** demonstrates the extreme variability in drogue tracks once a particle leaves the nearshore zone and enters the influence of the inlet. The figure plots the movements of all drogues for the entire simulation. For reference, **Figure**

11 plots the path of drogue A for the entire monitoring period. The particle pathway suggests that once the drogue enters the inlet it travels throughout the dominant tidal range of the inlet traversing a path through the estuary, about 7-8 miles upriver, and into the open ocean along the ebb tidal platform.

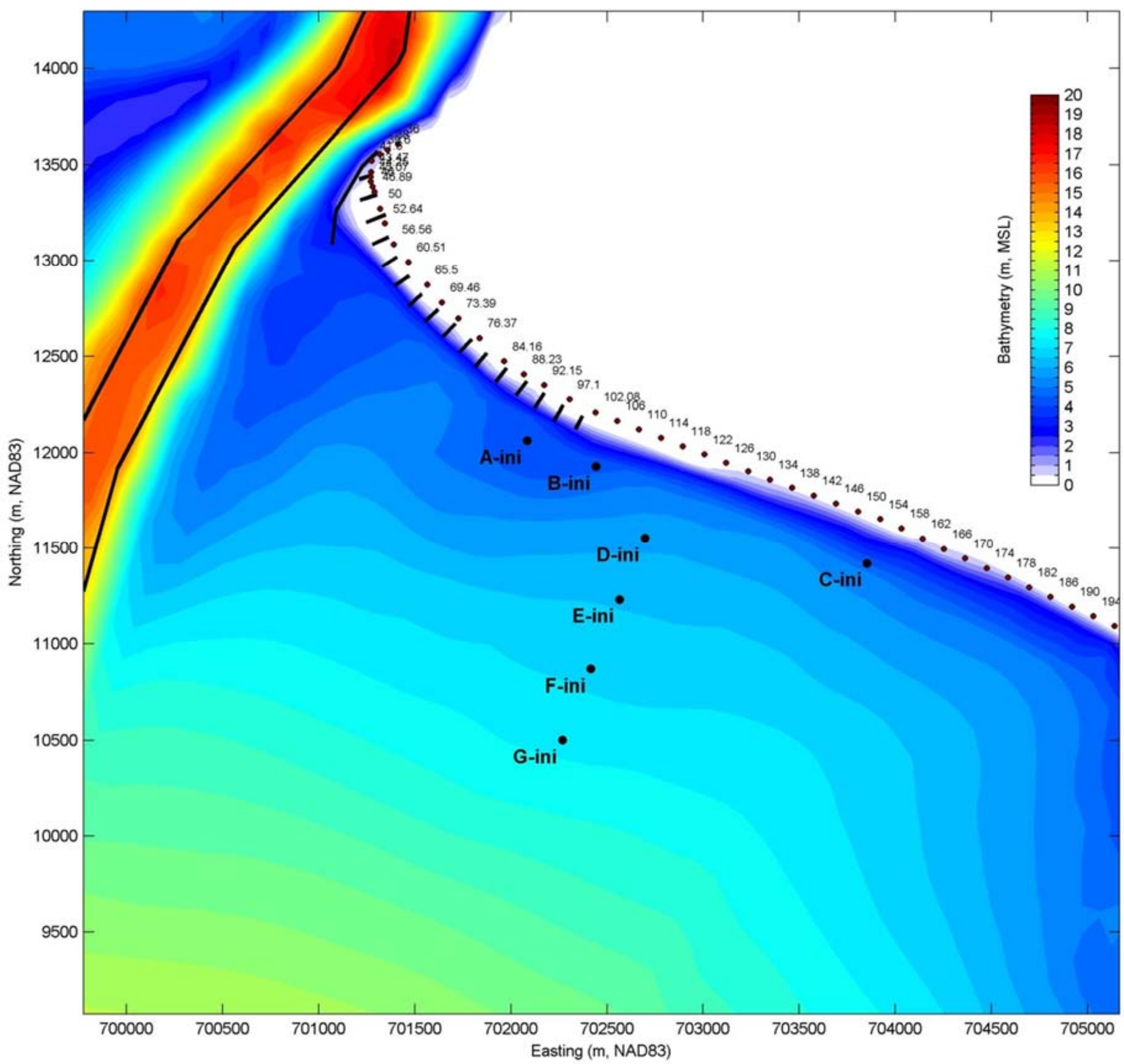

Figure 9: Initial deployment of each drogue tacked for this analysis.

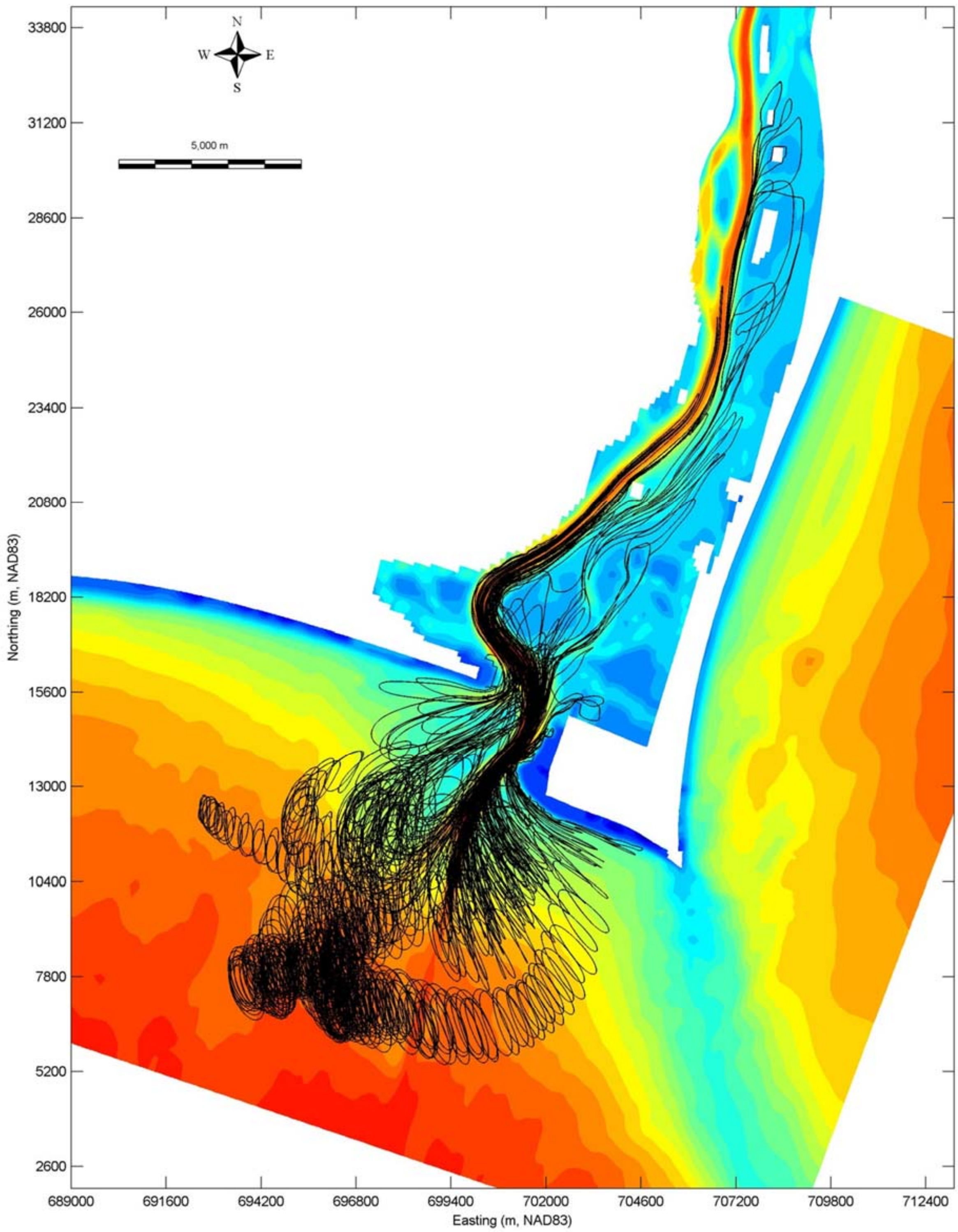

Figure 10: All drogue tracks for the entire monitoring period.

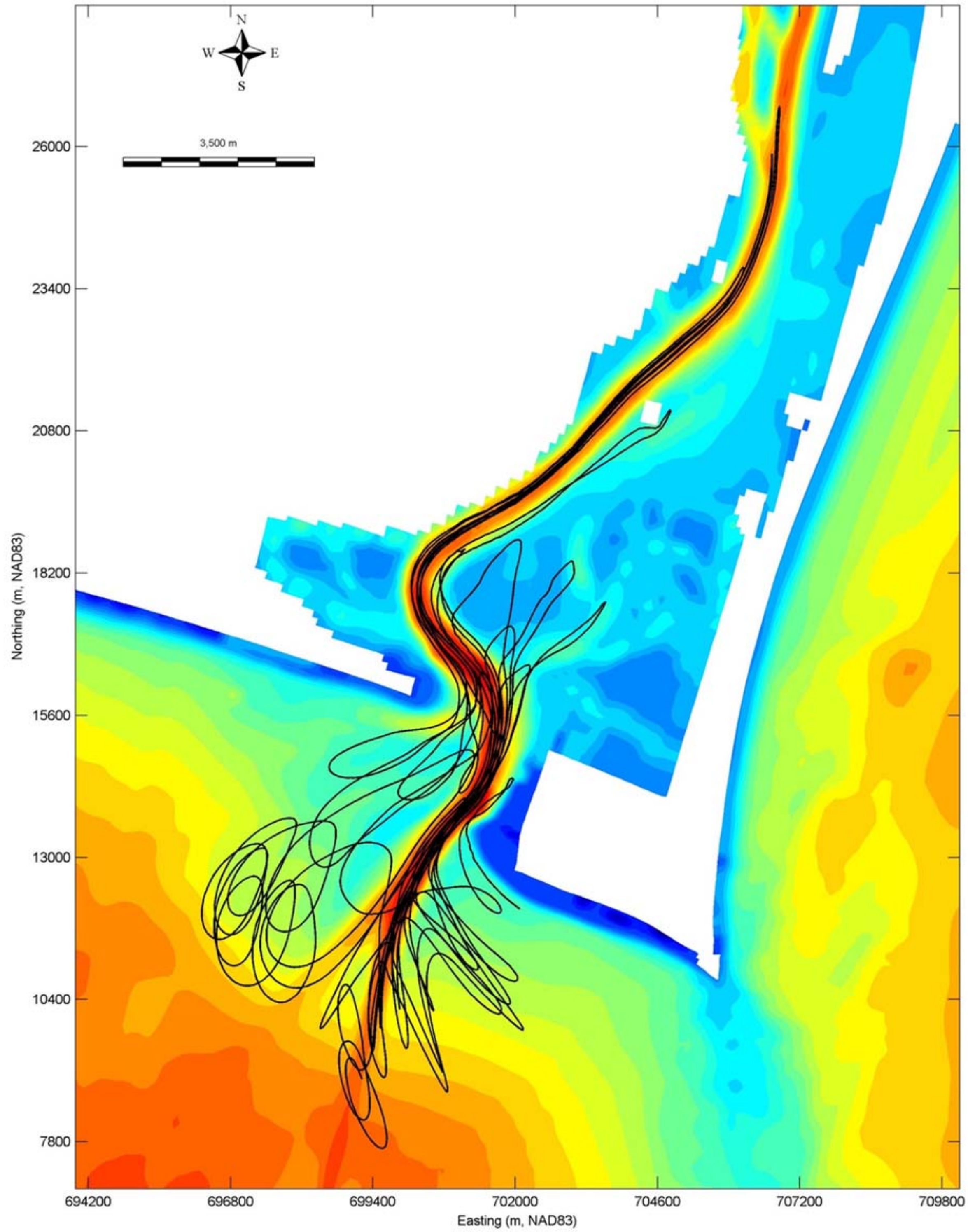

Figure 11: Path of drogue ‘A’ for the entire monitoring period.

Summary results for each drogue are tabulated in **Tables 1** and **2** for neap and spring tide drogue releases, respectively. The tabular results indicate the total number of model time steps required for the drogue to reach the inlet along with the total travel time, in hours. Each time step represents 0.2 minutes, or 12 seconds in the numerical model. The difference between the beach fill only and with terminal groin travel times is additionally noted. Negative times suggest longer travel times under the with terminal groin condition.

Table 1: Drogue travel times when released during a neap tide.

Drogue ID	Fill Only		Terminal Groin w/ Fill		Difference
	No. Time Steps	Time (hrs)	Time Steps	Time (hrs)	(hrs)
A	1,840	6.1	1,855	6.2	-0.05
B	1,975	6.6	1,990	6.6	-0.05
C	9,075	30.3	9,360	31.2	-0.9
D	2,385	8.0	2,425	8.1	-0.1
E	2,620	8.7	2,625	8.8	-0.02
F	2,920	9.7	2,920	9.7	0.0
G	5,820	19.4	5,800	19.3	0.1

Table 2: Drogue travel times when released during a spring tide.

Drogue ID	Fill Only		Terminal Groin w/ Fill		Difference
	No. Time Steps	Time (hrs)	Time Steps	Time (hrs)	(hrs)
A	290	1.0	330	1.1	-0.1
B	455	1.5	580	1.9	-0.4
C	10,300	34.3	17,710	59.0	-24.7
D	730	2.4	950	3.2	-0.7
E	3,070	10.2	3,320	11.1	-0.8
F	3,520	11.7	3,600	12.0	-0.3
G	3,780	12.6	3,820	12.7	-0.1

The tracking results suggest that the travel time from the nearshore off Bald Head Island to the inlet is, generally speaking, very modestly slowed following the construction of a beach fill with a terminal groin. There were two exceptions to this finding whereby drogue releases F and G on a neap tide experienced either no change or a slight decrease in travel time following groin construction. Typically drogues released during a spring tide were slowed slightly more than those released during a neap tide. In either case, with the exception of one outlier (drogue C), these differences were very modest. The data suggest that, on average, drogue travel was slowed by about 0.16 hours (9.6 minutes) for the neap tide releases. For the spring tide releases, travel time was slowed by an average of about 3.9 hours under with groin conditions. The larger spring tide difference is wholly attributable to drogue C initially located at the eastern boundary of tidal influence. This drogue tended to slow primarily near the intertidal beach under with terminal groin conditions resulting in an abnormally large delay of about 24.7 hours for drogue C. Possible reasons for the performance of drogue C on a spring tide are discussed below.

Neap Tide Releases. **Figures 12** through **18** compare individual drogue tracks computed under with and without terminal groin conditions for drogues released during a neap tide condition. The time required to reach the inlet is noted on each figure along with the tidal phase at Southport during the period of measurement. Travel times to the inlet varied between 6.1 and 31.2 hours typically corresponding with initial distance from the inlet. Differences in travel time with and without the terminal groin varied between 3 and 57 minutes and also typically correlate with the distance from the inlet. As previously stated, the average time difference potentially attributable to the terminal groin was less than 10 minutes indicating the structure is not expected to significantly hinder the timely ability of a nearshore particle to reach the inlet. Travel directions between with and without groin simulations typically deviated only near the inlet itself as flows are diverted both around (and weakly through) the pre-filled, porous terminal groin rather than being carried directly around the sandy shoreline of the Point of Bald Head Island.

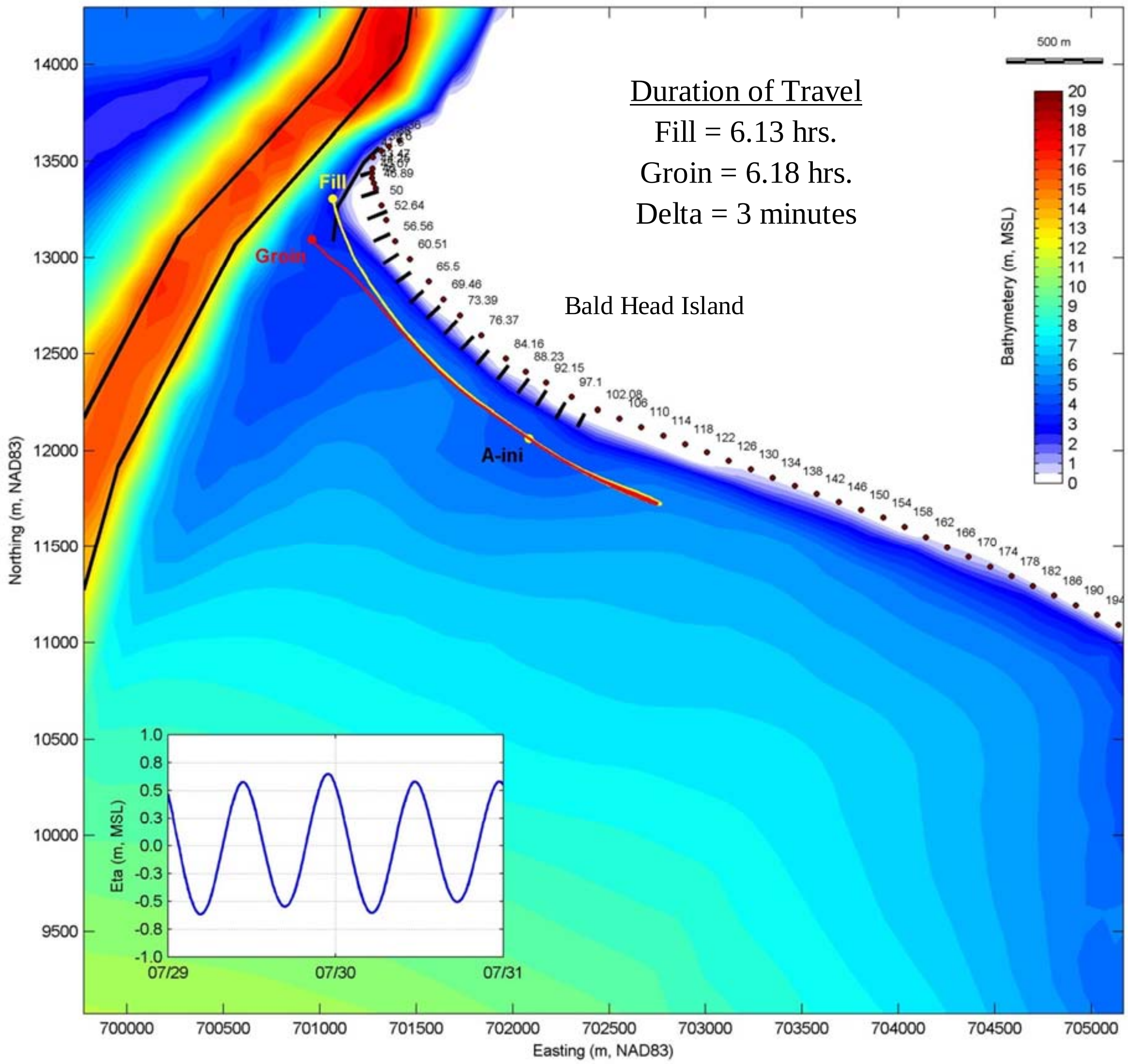

Figure 12: Drogue track A from deployment to inlet, with and without the terminal groin.

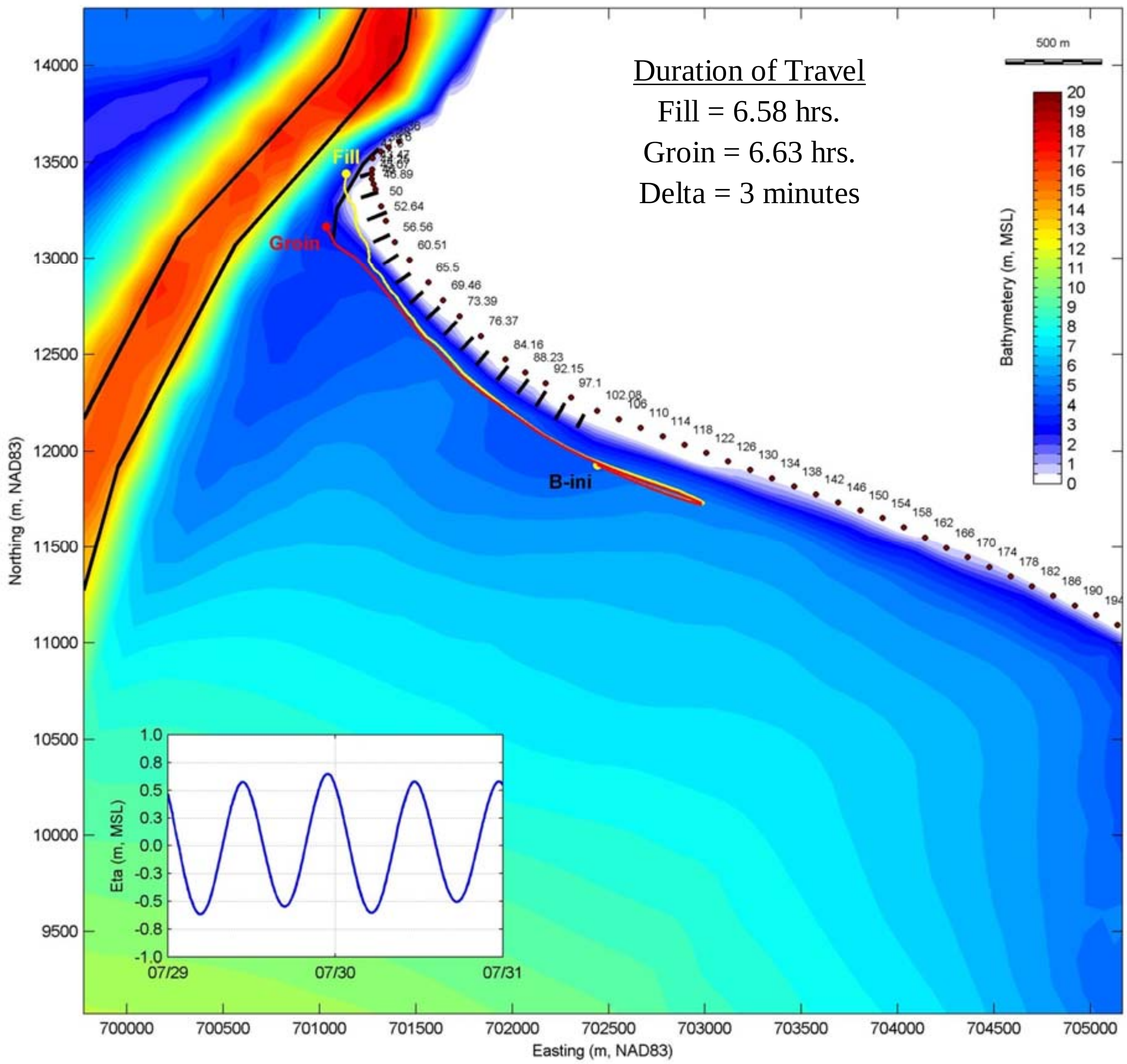

Figure 13: Drogue track B from neap tide deployment to inlet, with and without the terminal groin.

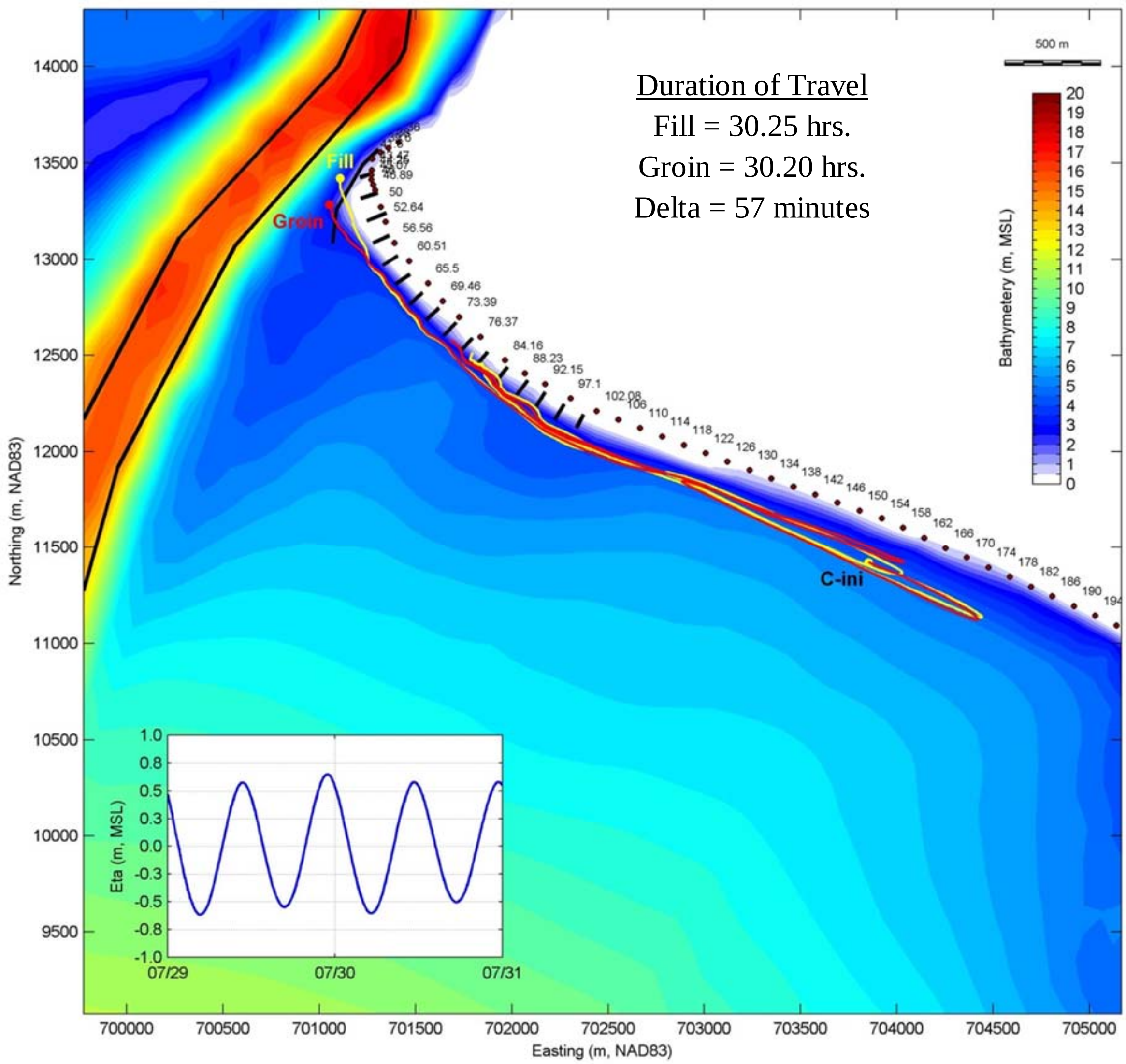

Figure 14: Drogue track C from neap tide deployment to inlet, with and without the terminal groin.

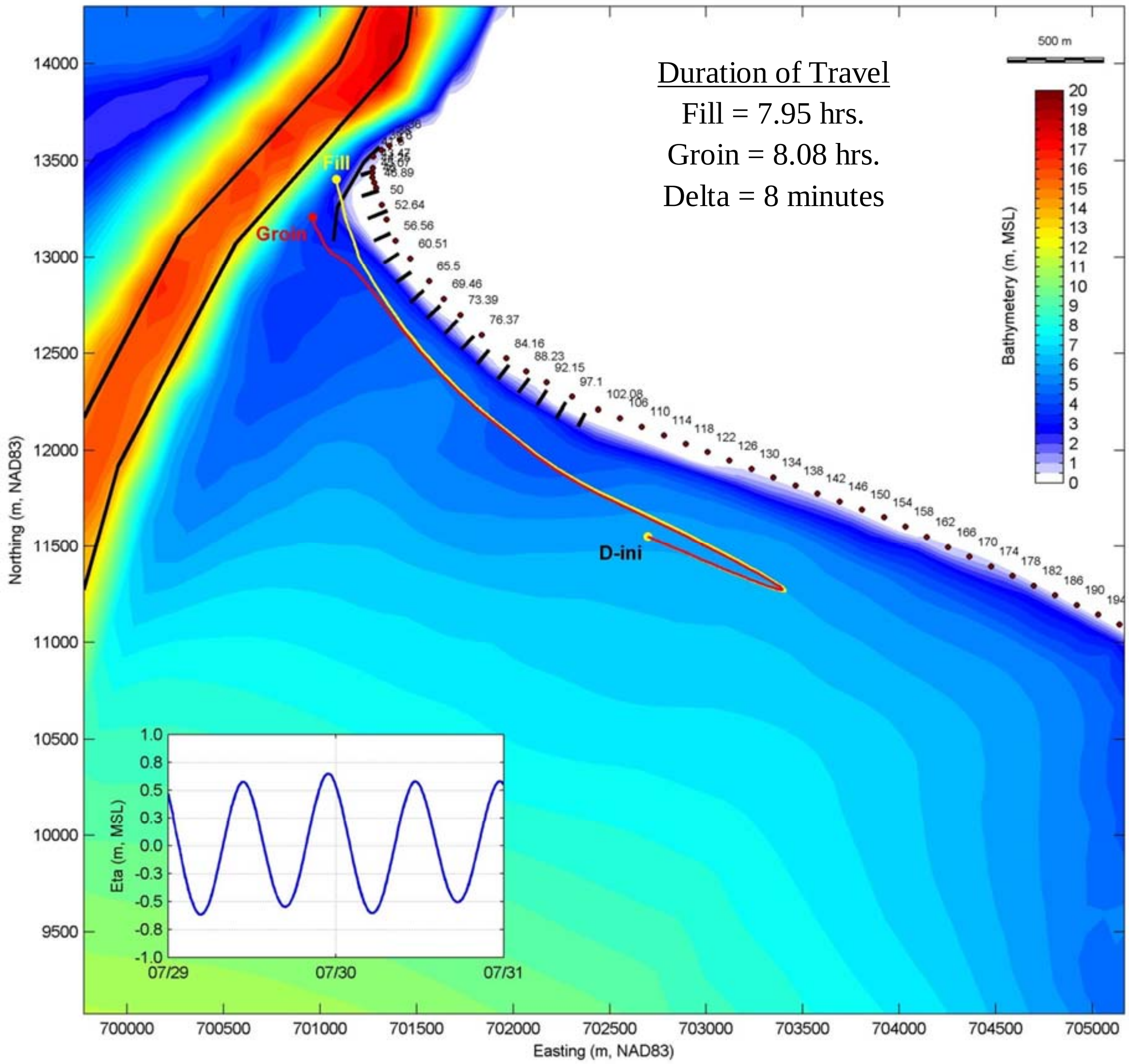

Figure 15: Drogue track D from neap tide deployment to inlet, with and without the terminal groin.

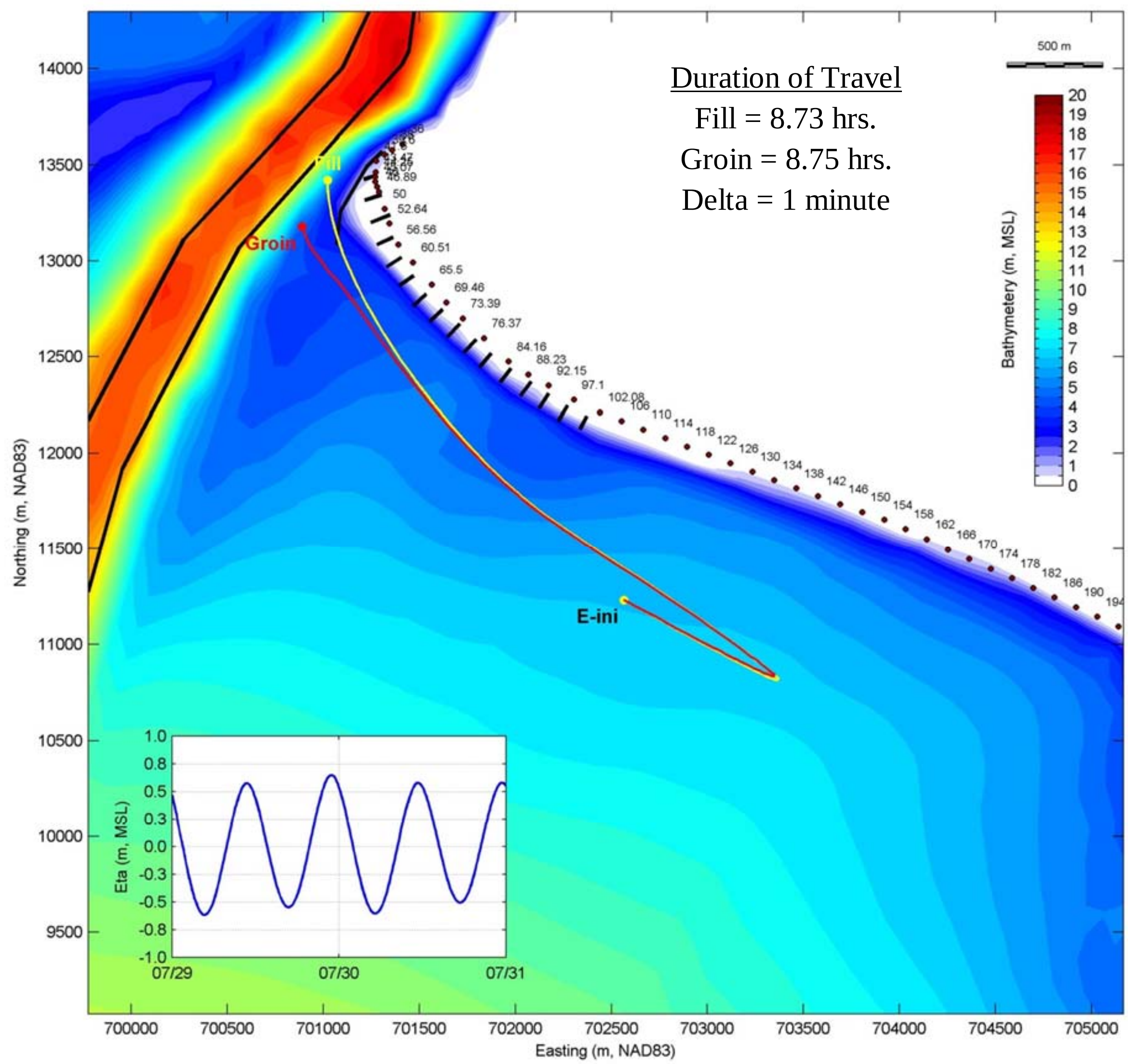

Figure 16: Drogue track E from neap tide deployment to inlet, with and without the terminal groin.

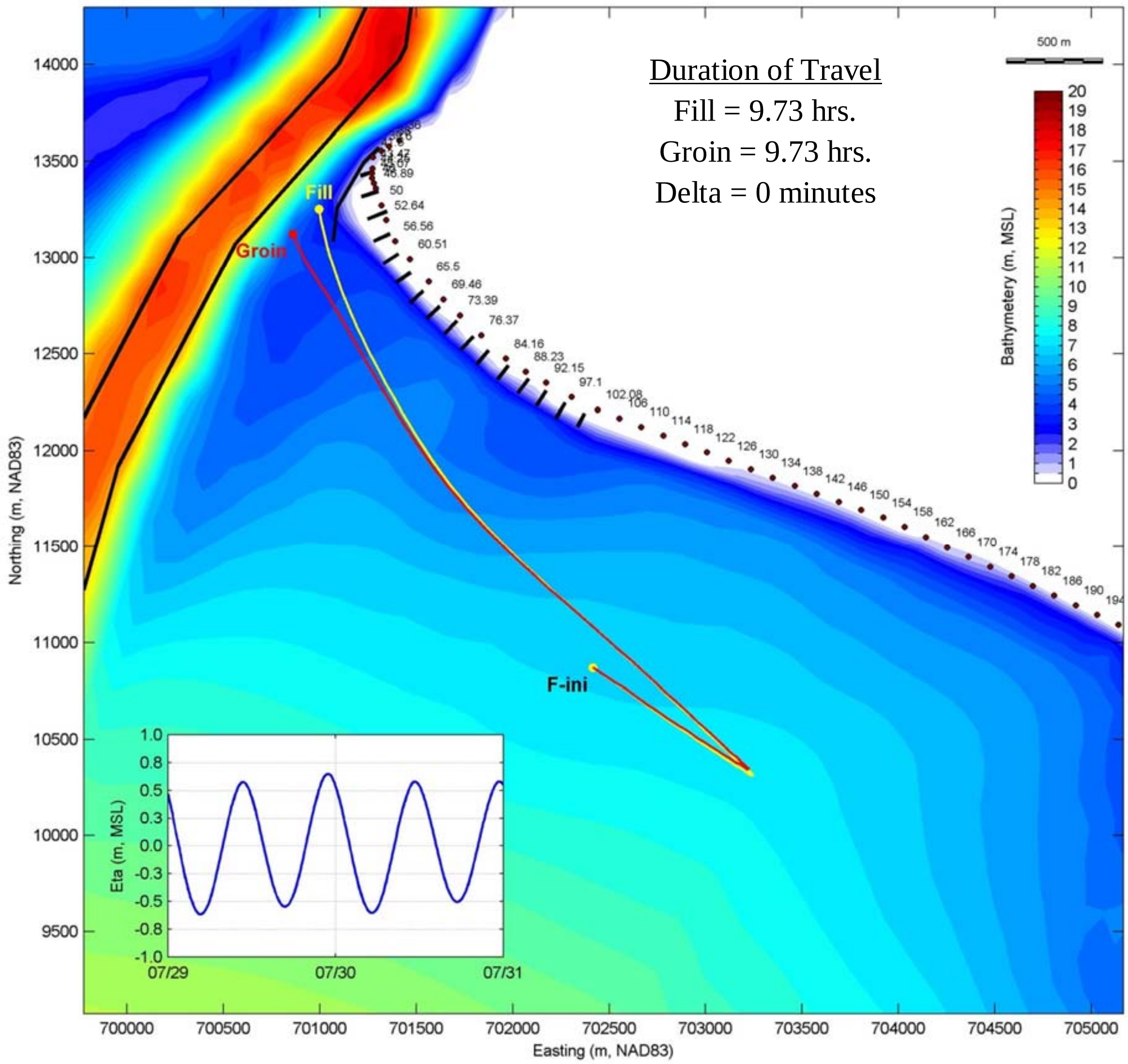

Figure 17: Drogue track F from neap tide deployment to inlet, with and without the terminal groin.

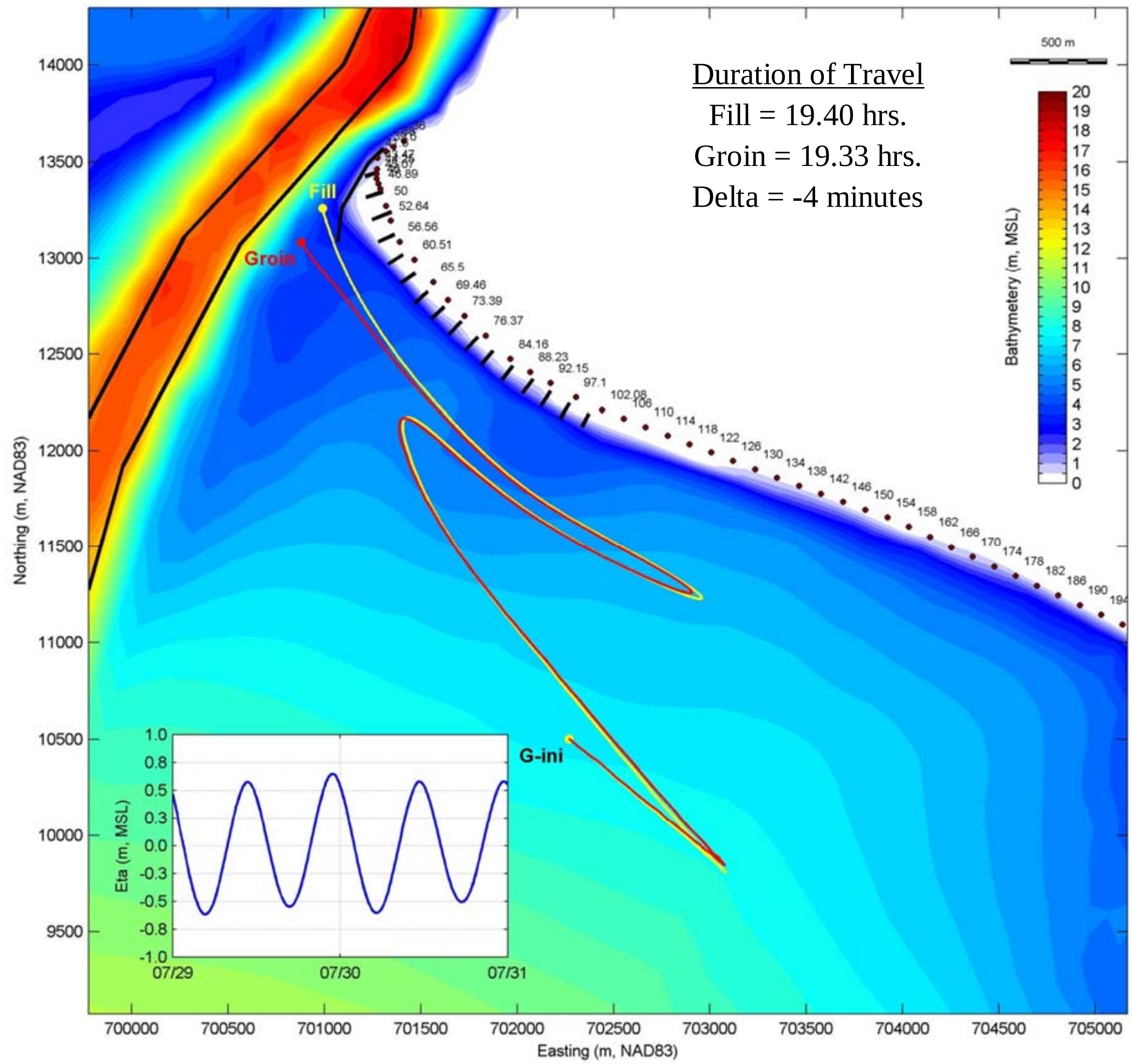

Figure 18: Drogue track G from neap tide deployment to inlet, with and without the terminal groin.

Spring Tide Releases. **Figures 19** through **25** compare individual drogue tracks computed under with and without terminal groin conditions for drogues released during a spring tide condition. The time required to reach the inlet is noted on each figure along with the tidal phase computed at Southport during the period of measurement. Travel times to the inlet varied between 1 and 59 hours again varying with respect to the distance from the inlet. Differences in travel time for with and without groin conditions varied between 8 minutes and 24.7 hours. Excluding that of drogue C (24.7 hours) differences in transit time following terminal structure construction range between 8 and 50 minutes, averaging about 25.2 minutes.

The large difference in transit time for drogue C is attributable to the fact that the particle managed to migrate onto the intertidal beach and effectively become 'stranded' significantly slowing the drouge's motion for a number of tidal oscillations – observable as the drogue path travels very near to the shoreline in the with groin scenario (see **Figure 21**). This stranding occurred east of station 130+00 where significant differences in the nearshore bathymetric profile are included in the model domain. These bathymetric variations are the result of differences in the beach fill sectional density as the beach fill is less voluminous to nonexistent here under without terminal groin conditions. The changes in travel time and particle path here are in response to nearshore bathymetric variations (i.e., less fill allowed the drogue to travel closer to shore and move more slowly) rather than hydraulic influences of the terminal structure. Once clear of this section of shoreline (west of station 130+00), the particles follow a similar path and timetable into the inlet.

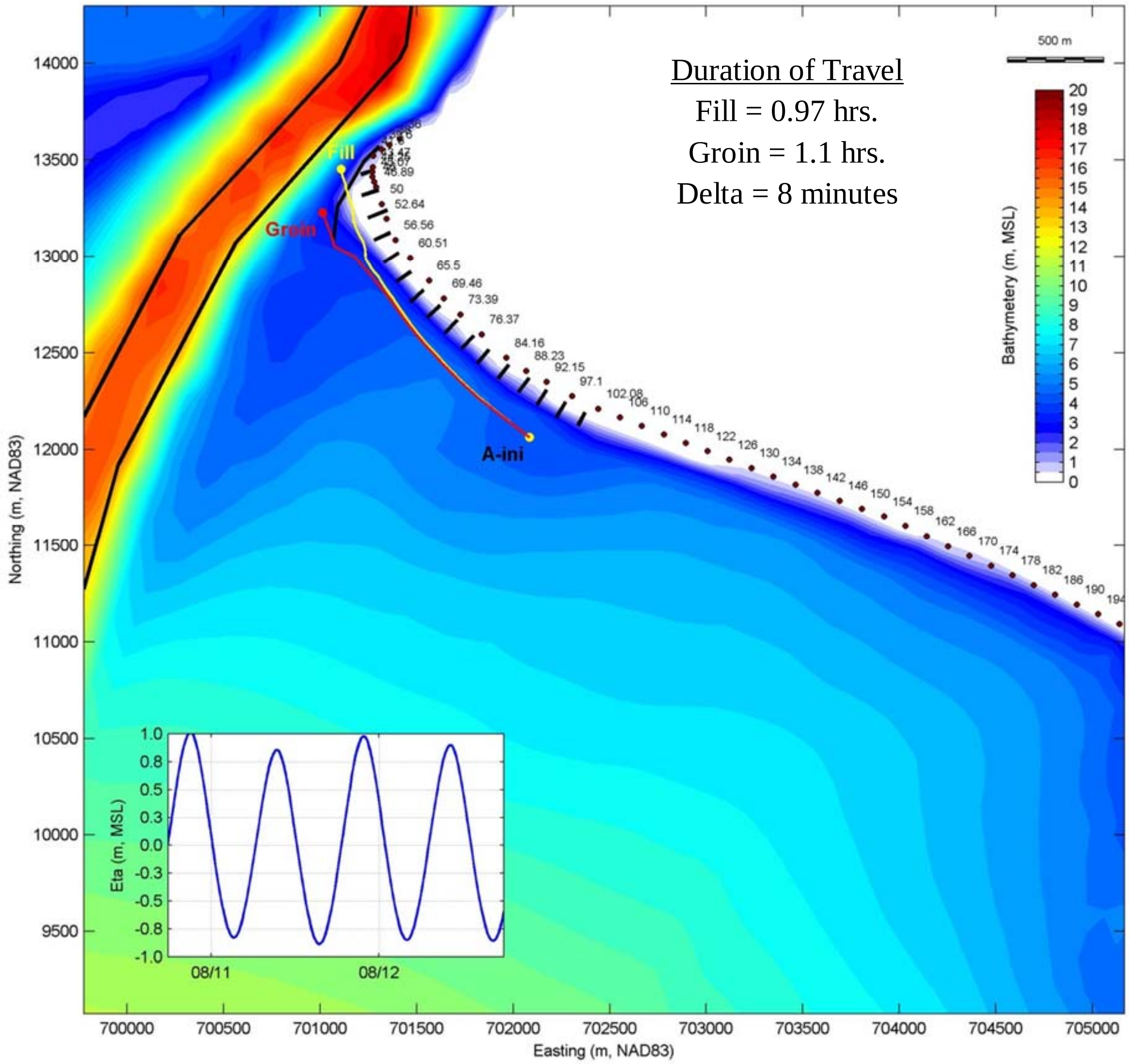

Figure 19: Drogue track A from spring tide deployment to inlet, with and without the terminal groin.

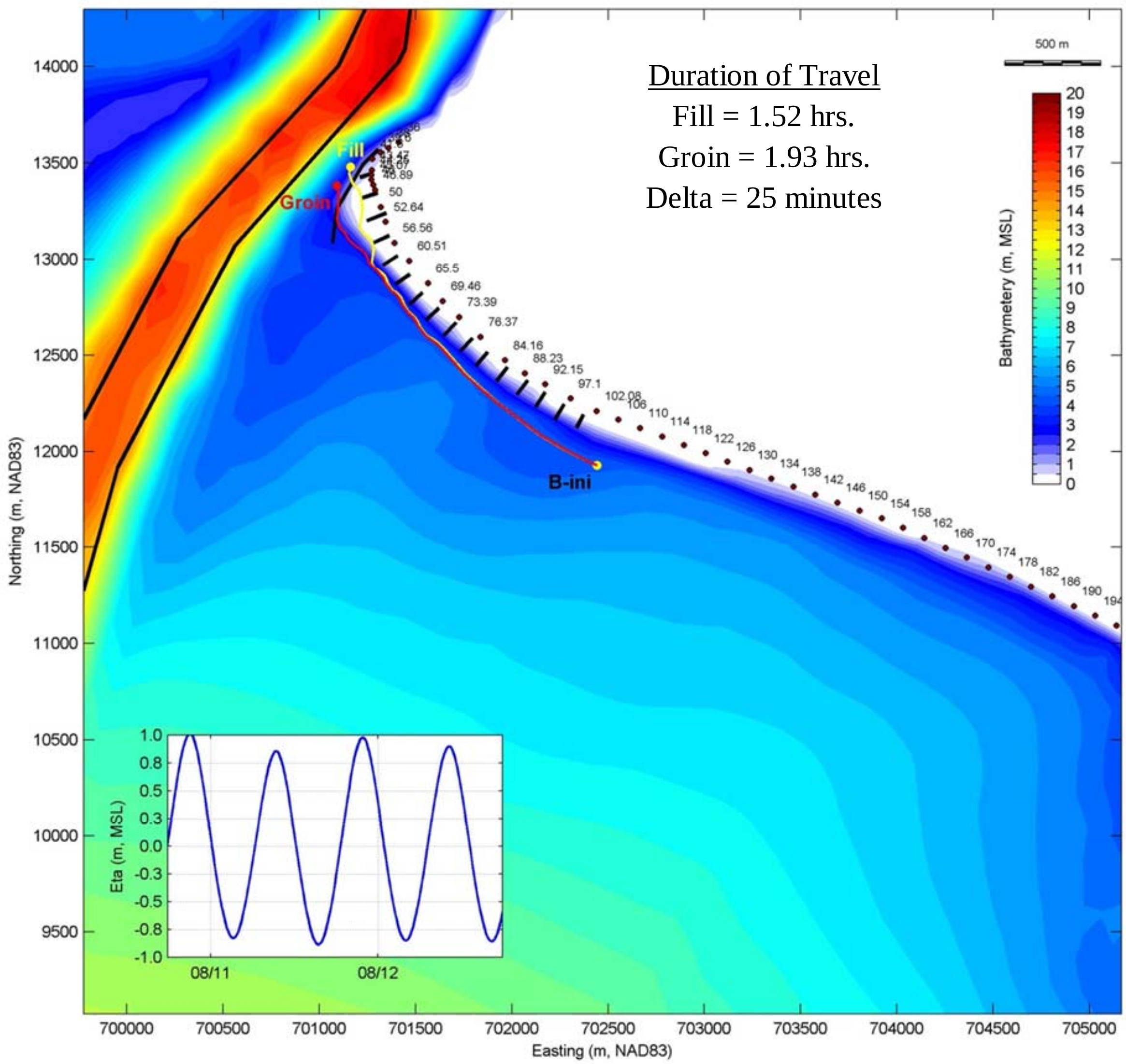

Figure 20: Drogue track B from spring tide deployment to inlet, with and without the terminal groin.

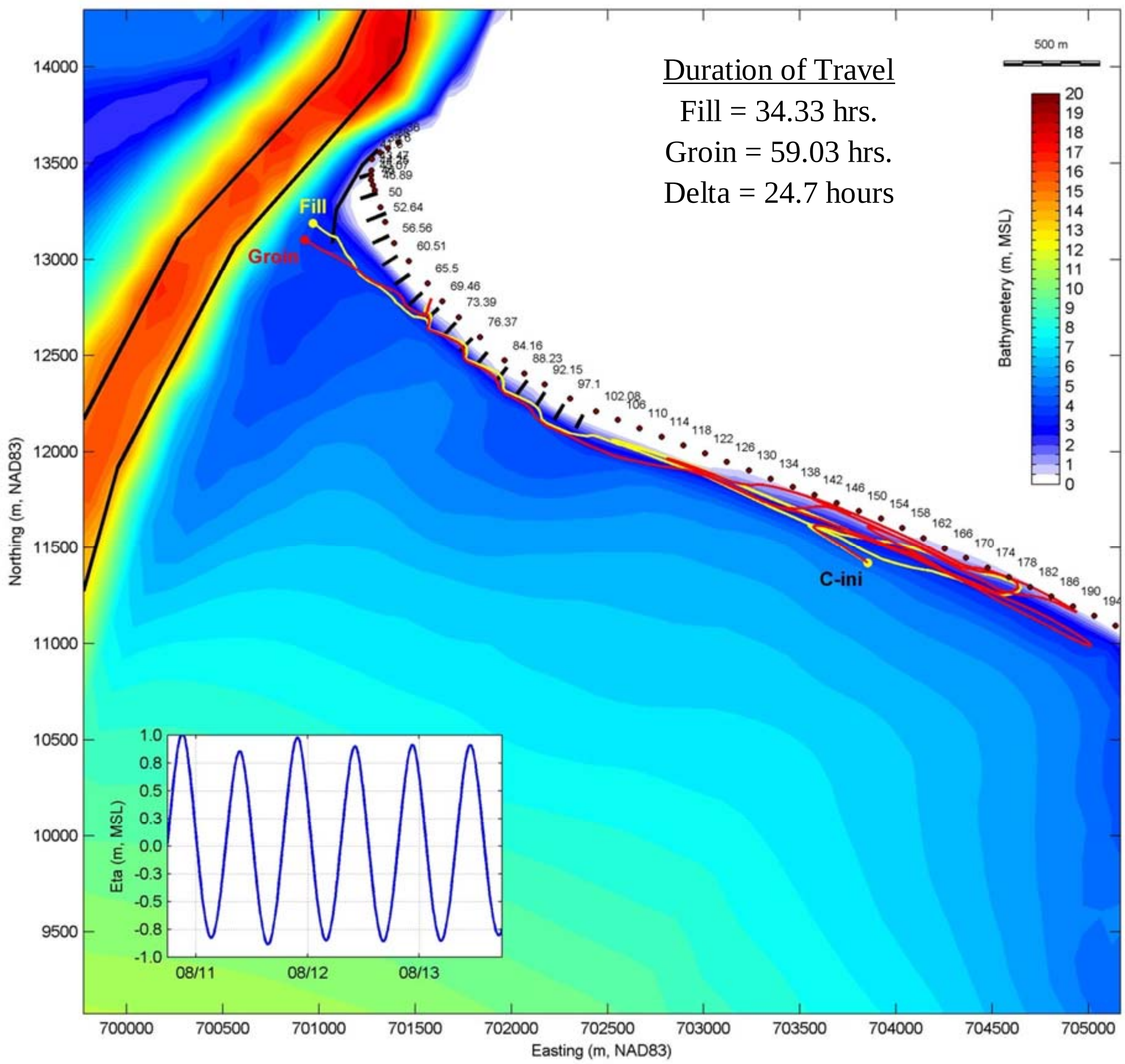

Figure 21: Drogue track C from spring tide deployment to inlet, with and without the terminal groin.

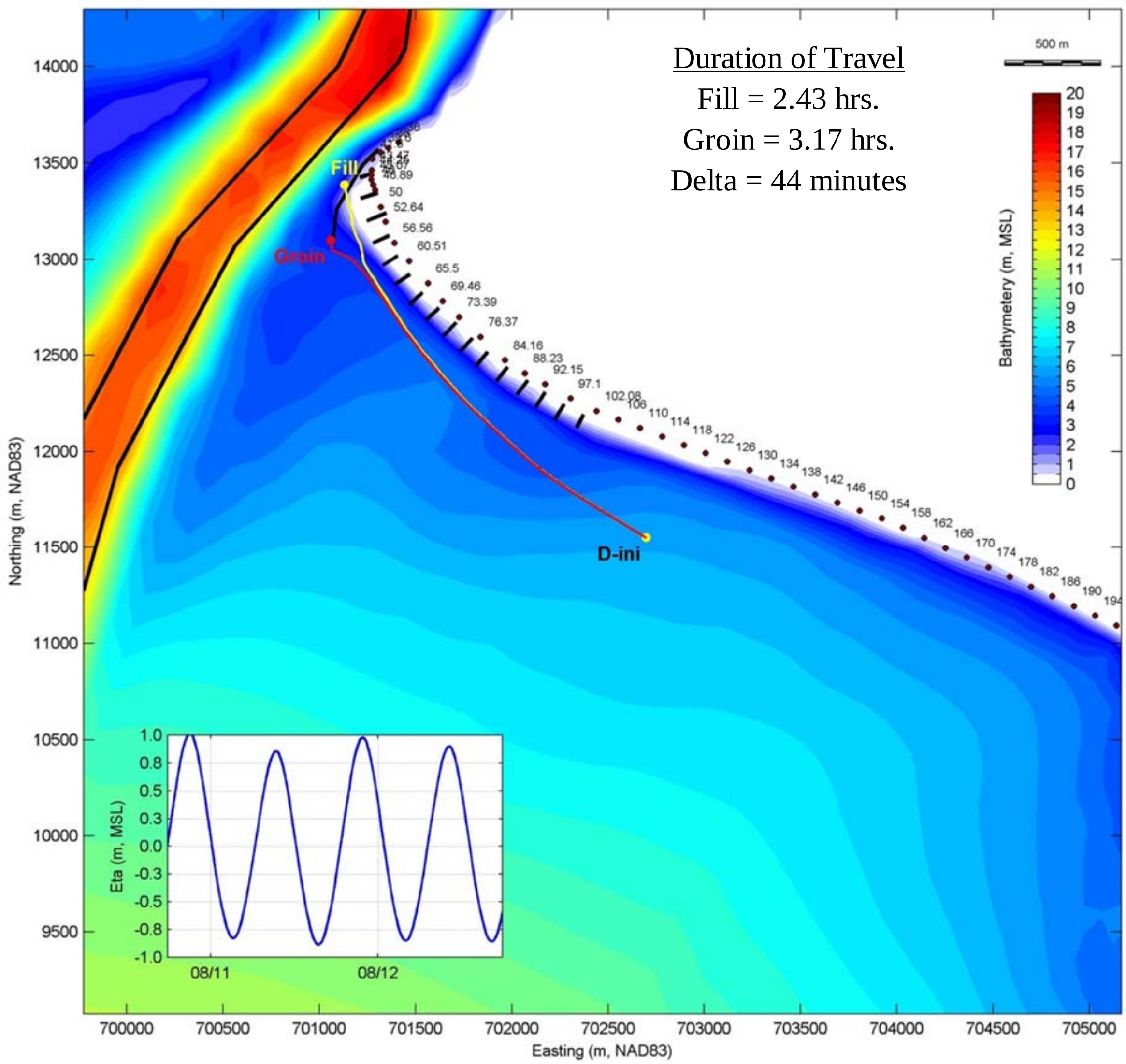

Figure 22: Drogue track D from spring tide deployment to inlet, with and without the terminal groin.

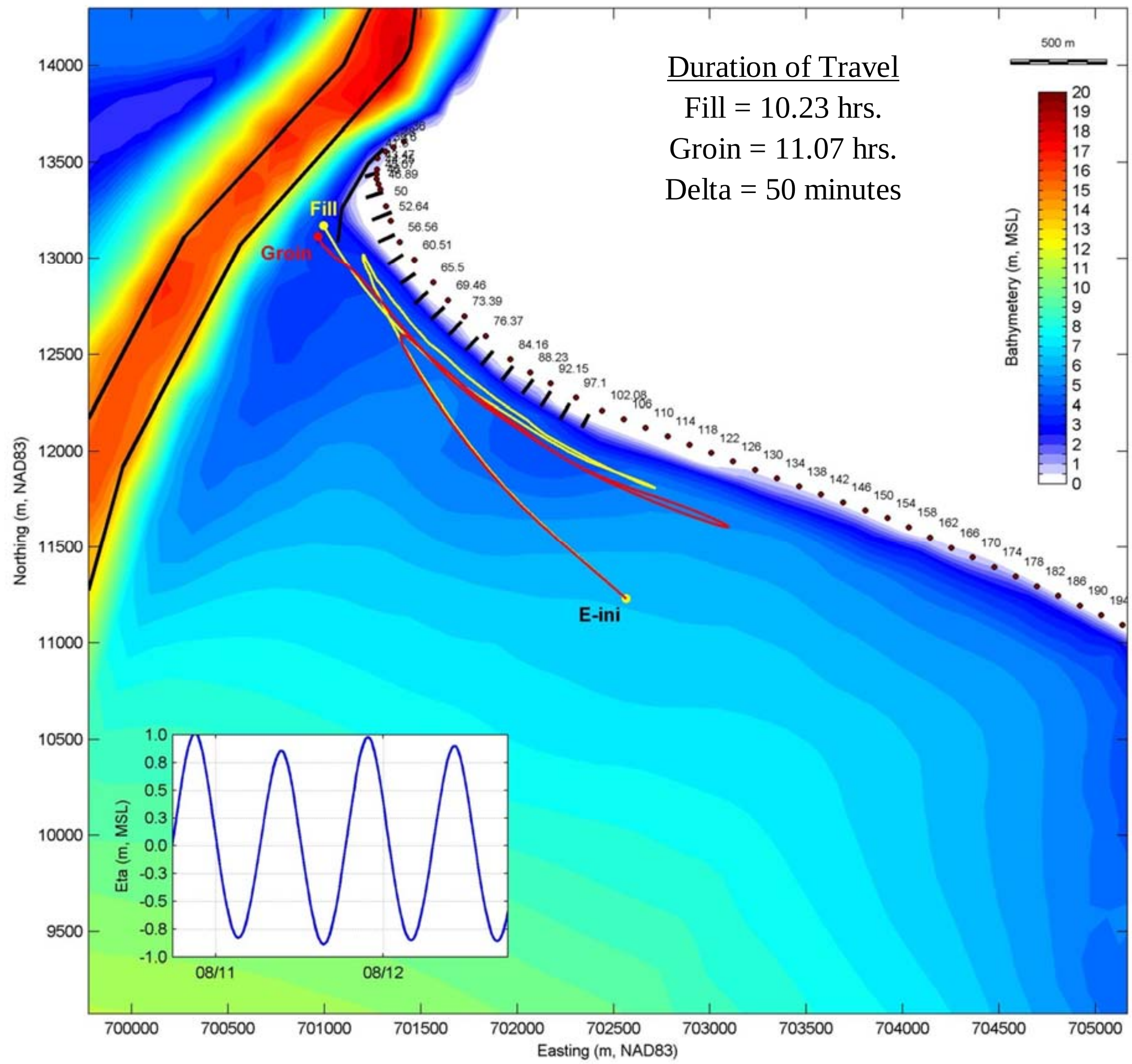

Figure 23: Drogue track E from spring tide deployment to inlet, with and without the terminal groin.

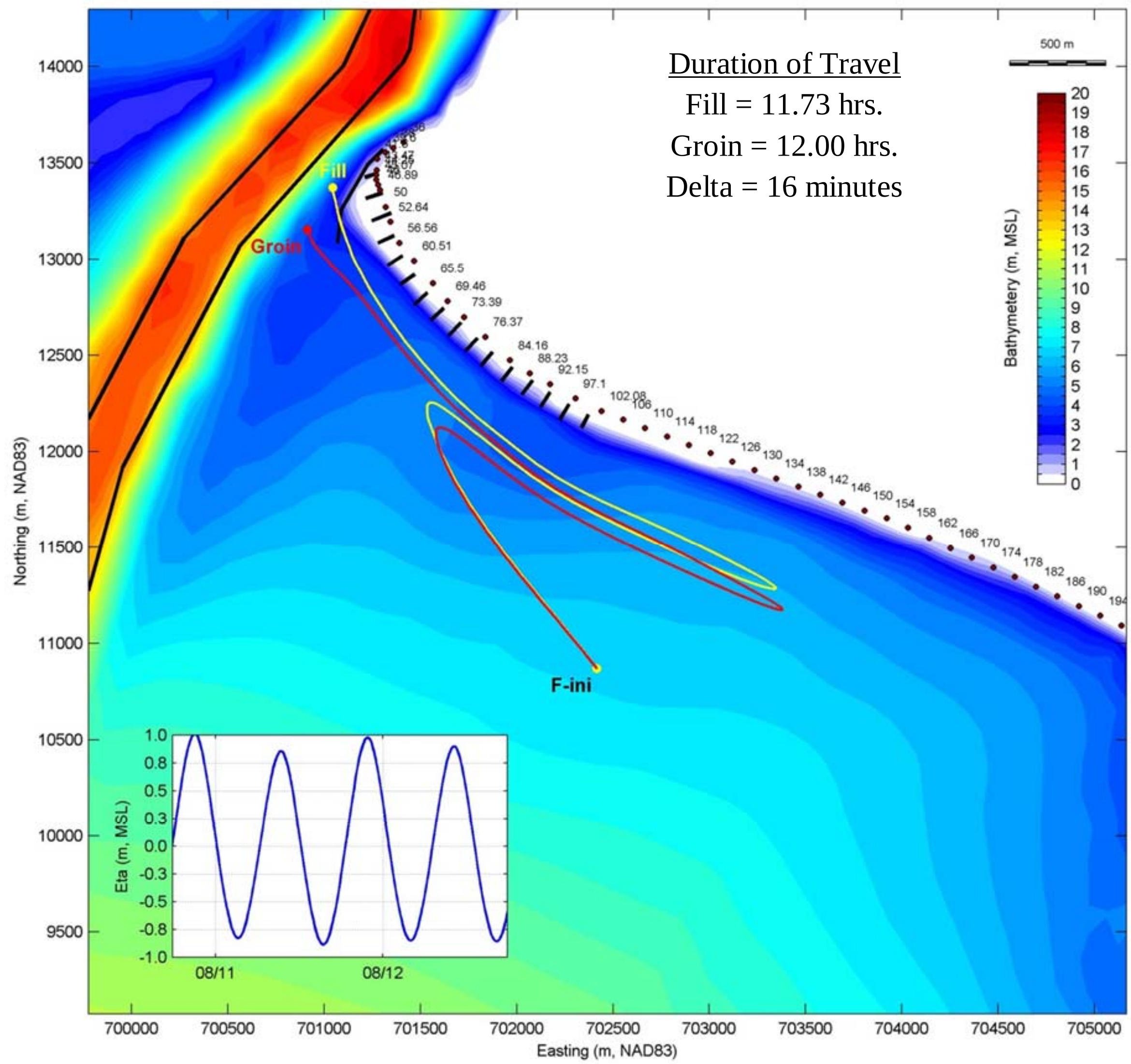

Figure 24: Drogue track F from spring tide deployment to inlet, with and without the terminal groin.

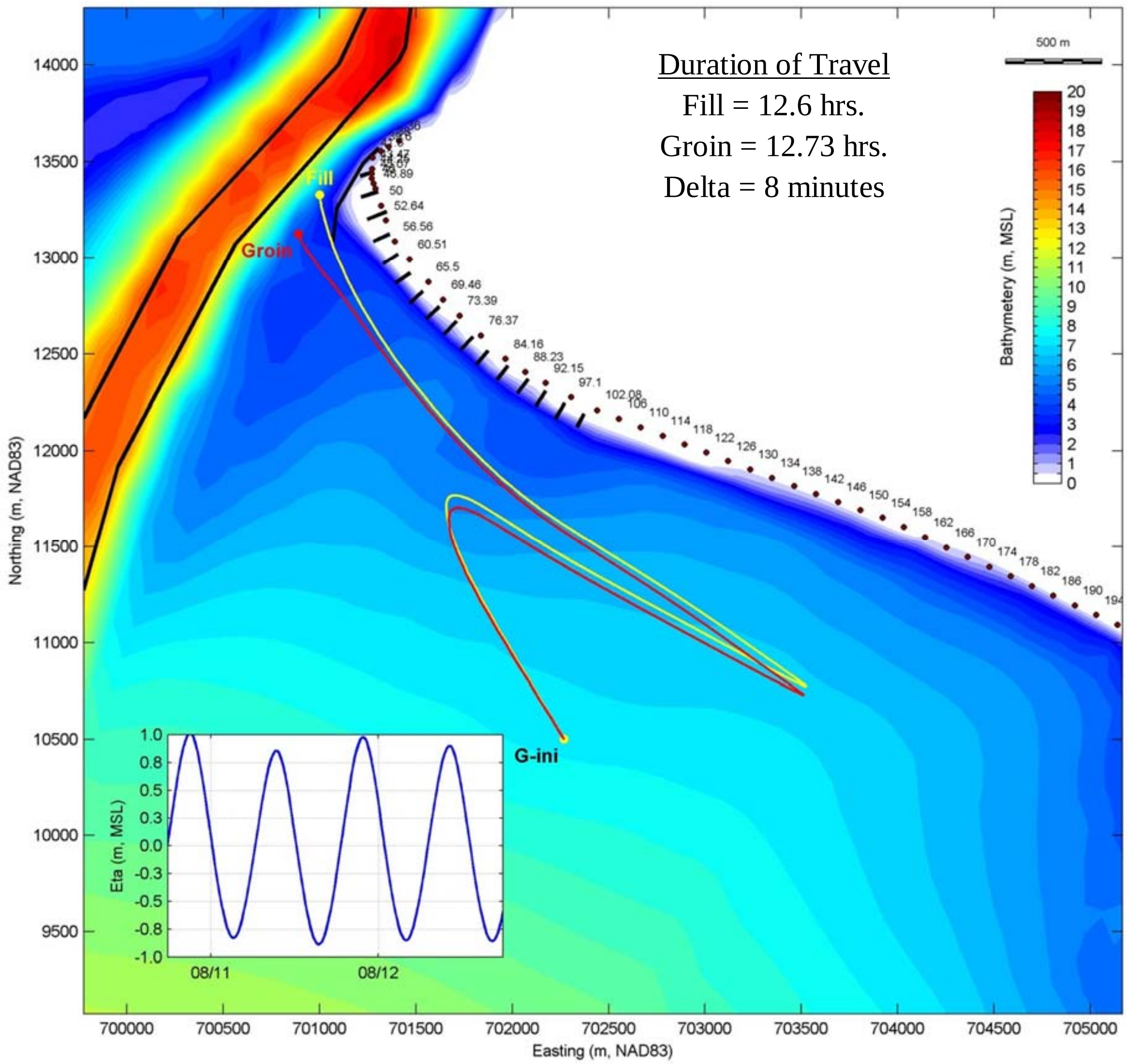

Figure 25: Drogue track G from spring tide deployment to inlet, with and without the terminal groin.

Particle Tracking. The Deflt3D particle tracking model was used to simulate the instantaneous release of a set number of particles contained in a specified amount of tracking agent. The particle tracking model is run independently of the hydrodynamic model and utilizes the hydrodynamic model results as input. Like the drogue tracking exercises, tracer particles are conservative in that there is no decay over time. Tracer particles were released twice, at time steps representing both spring and neap tide conditions and tracked throughout the remaining simulation run. The timing of tracer deployment was the same as used for the drogue analyses. The total number of particles was specified at 10,000 and the total mass of tracer was 2 kg. Particles were released east of the groin field and are represented and mapped as concentrations.

Neap Tide Condition. **Figures 26** through **33** plot the particle distribution at various intervals in time following neap tide insertion. In each figure, the beach fill only and the fill with terminal groin alternatives are plotted side by side one another in order to yield a comparative view at a given time step. The figures plot only the particle positions through the fifth day following initial release given that by day five the particles are quite well distributed throughout the predominantly tidally influenced areas of the model. The tidal stage is indicated by the red line on the water level plot in the upper left corner of each figure. The dominant current direction (ebb or flood) is denoted on each figure by the large red arrow.

The results suggest few significant differences in the range and concentrations of particles through time. The with-terminal groin result does indicate initial higher concentrations of particles in the intertidal nearshore principally east of the beach fill limit. The apparent stranding of particles in the intertidal beach here is consistent with the drogue tracking result. As the tracer particles begin to mobilize into the inlet, increased particle concentrations along this reach subside and gain consistency with the fill only concentrations within about two days following insertion.

Spring Tide Condition. **Figures 34** through **41** plot the particle distribution at various intervals in time following spring tide insertion. The results for both spring and neap tide insertion times are similar in that the terminal groin appears to have little influence over the transport patterns of the tracer particles. Specifically, under both conditions, particles which enter the inlet on a flood tide and do not enter the very shallow portions of the estuary are subsequently mobilized offshore on the following ebb tide. A portion of these particles are returned into the inlet on the following flood tide(s) eventually becoming well distributed throughout the river, estuary, and marsh areas after only a few days. Alternatively stated, the large scale motion paths of the particles appear to generally follow pathways similar to those computed for the residual tides shown in **Figures 3** and **4**. The presence of the terminal groin appears to have no significant limiting influence on the ability of particles to enter the estuary and ebb/flood transport pathways described above. The size of the modeled terminal groin pales in scale to that of the overall range of distributed particles the spatial extent of which does not materially differ between with and without terminal groin conditions.

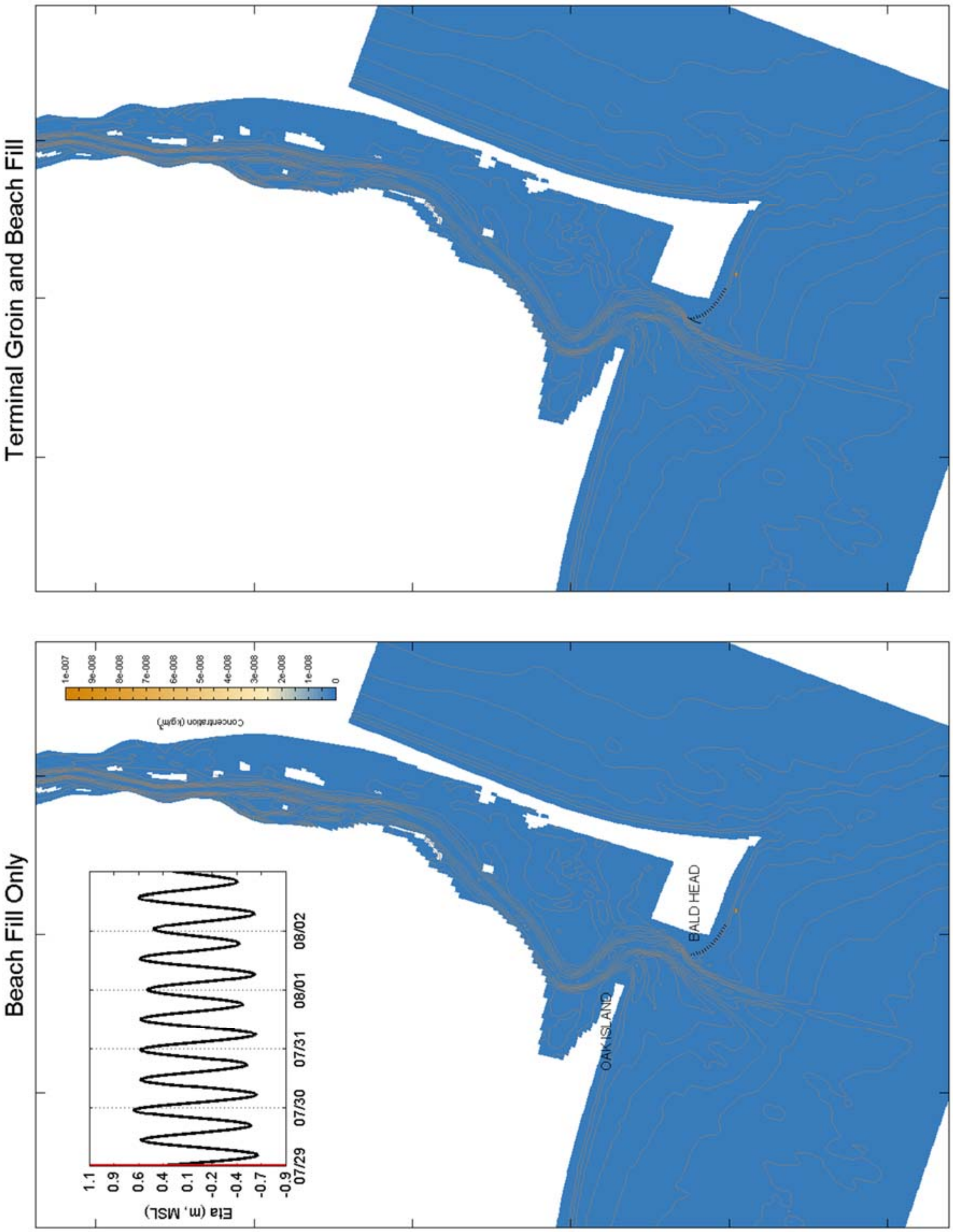

Figure 26: Particle concentration map 0 days following neap tide insertion.

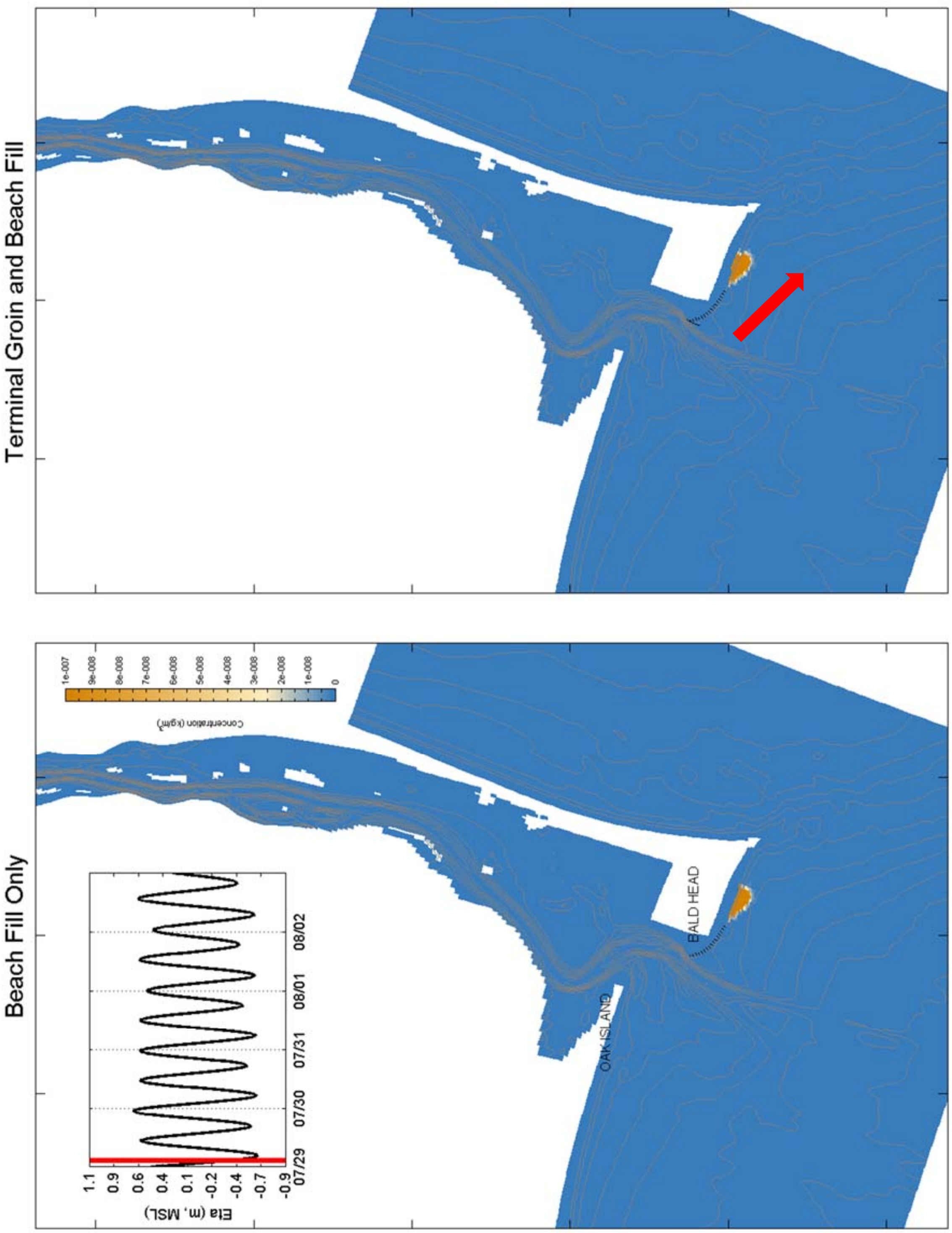

Figure 27: Particle concentration map hours following neap tide insertion.

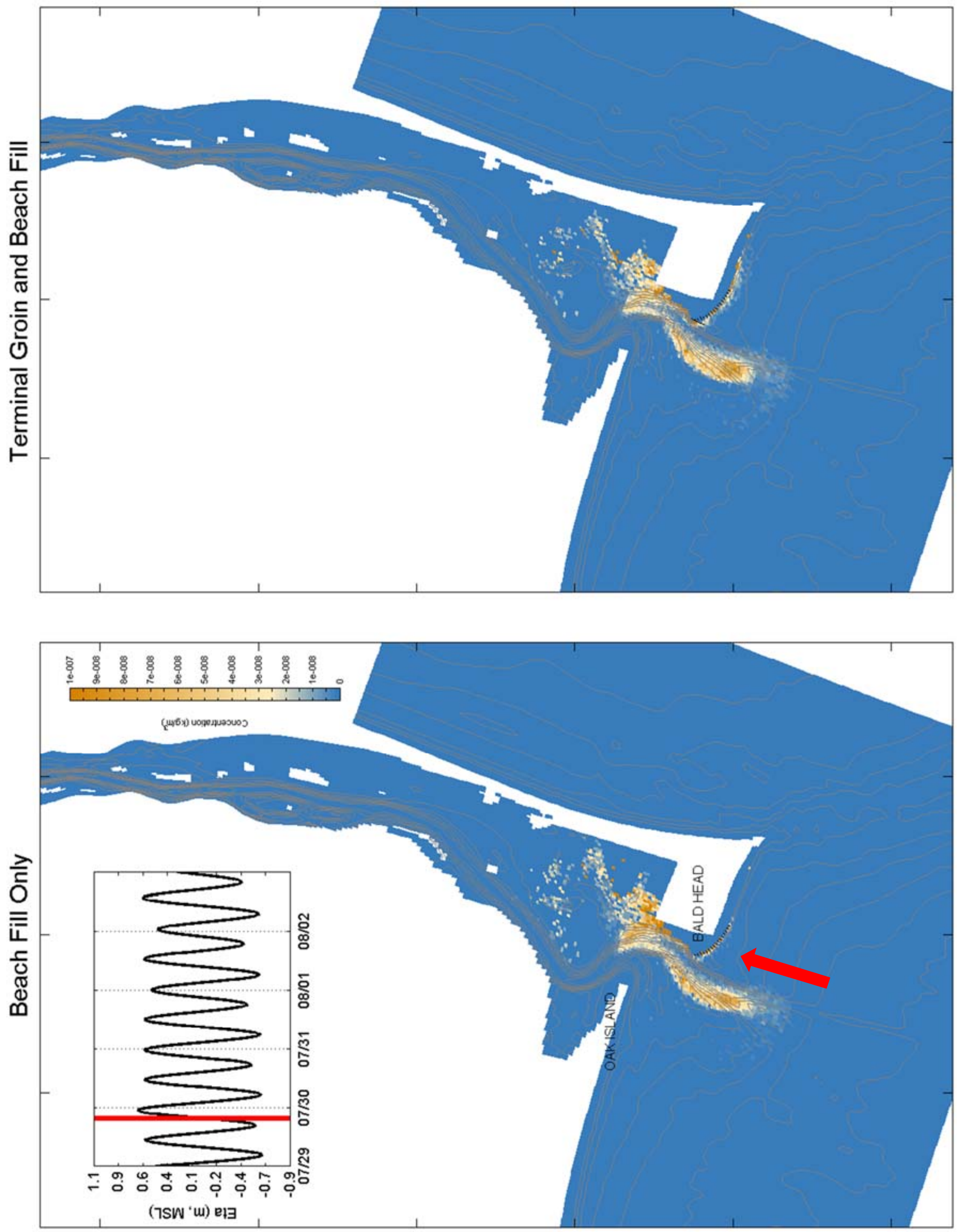

Figure 28: Particle concentration map about 1 day following neap tide insertion.

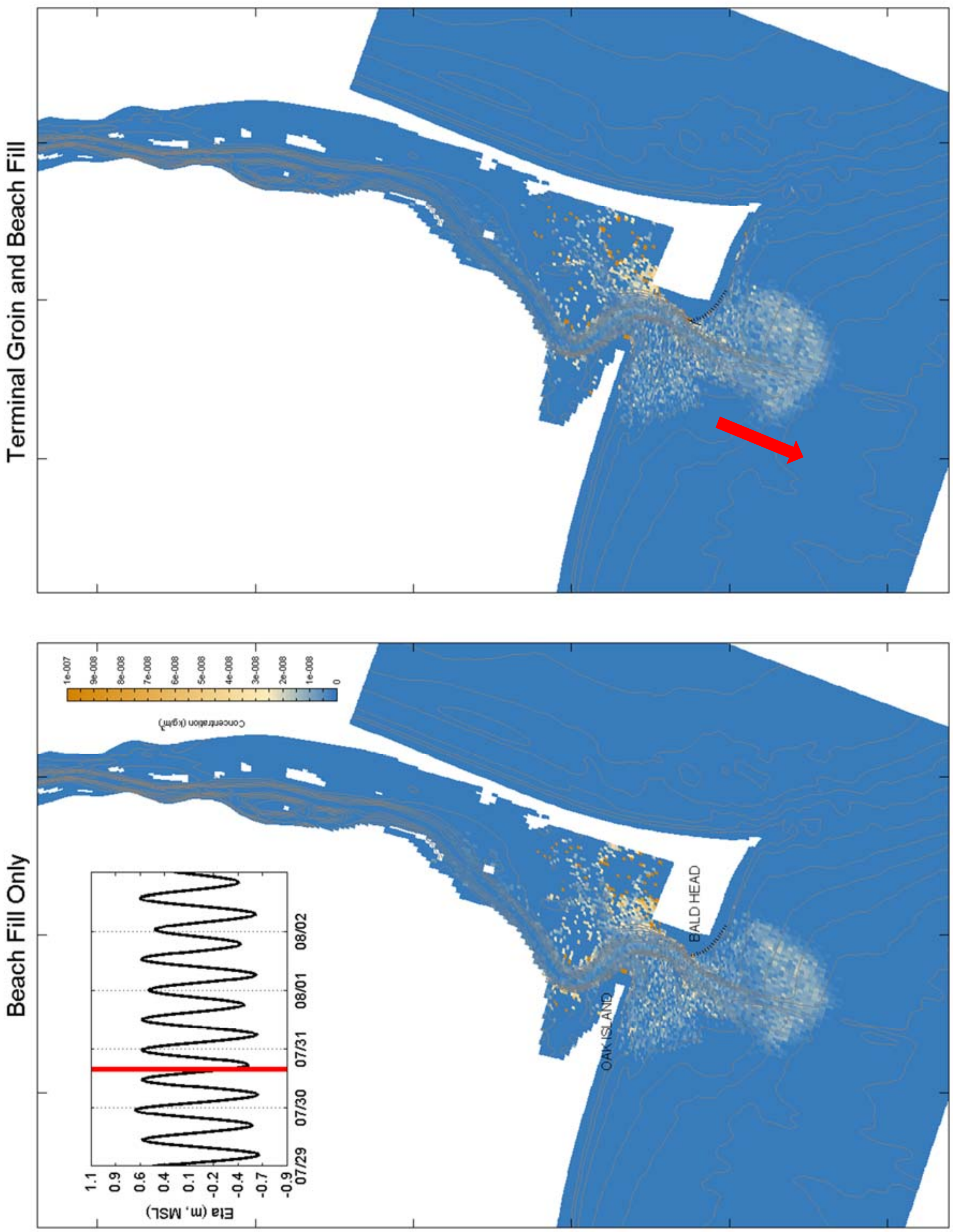

Figure 29: Particle concentration map about 1.7 days following neap tide insertion.

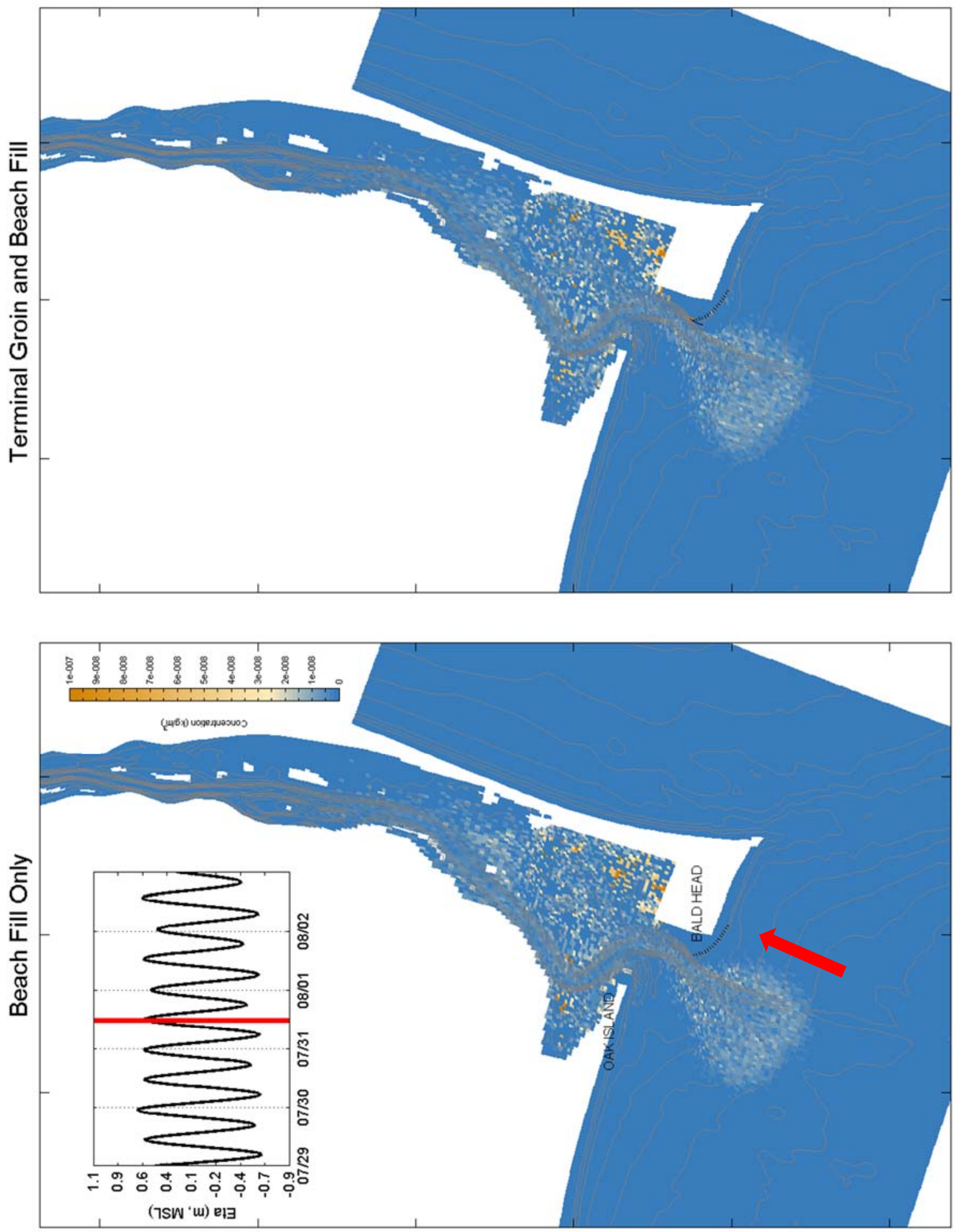

Figure 30: Particle concentration map about 2.5 days following neap tide insertion.

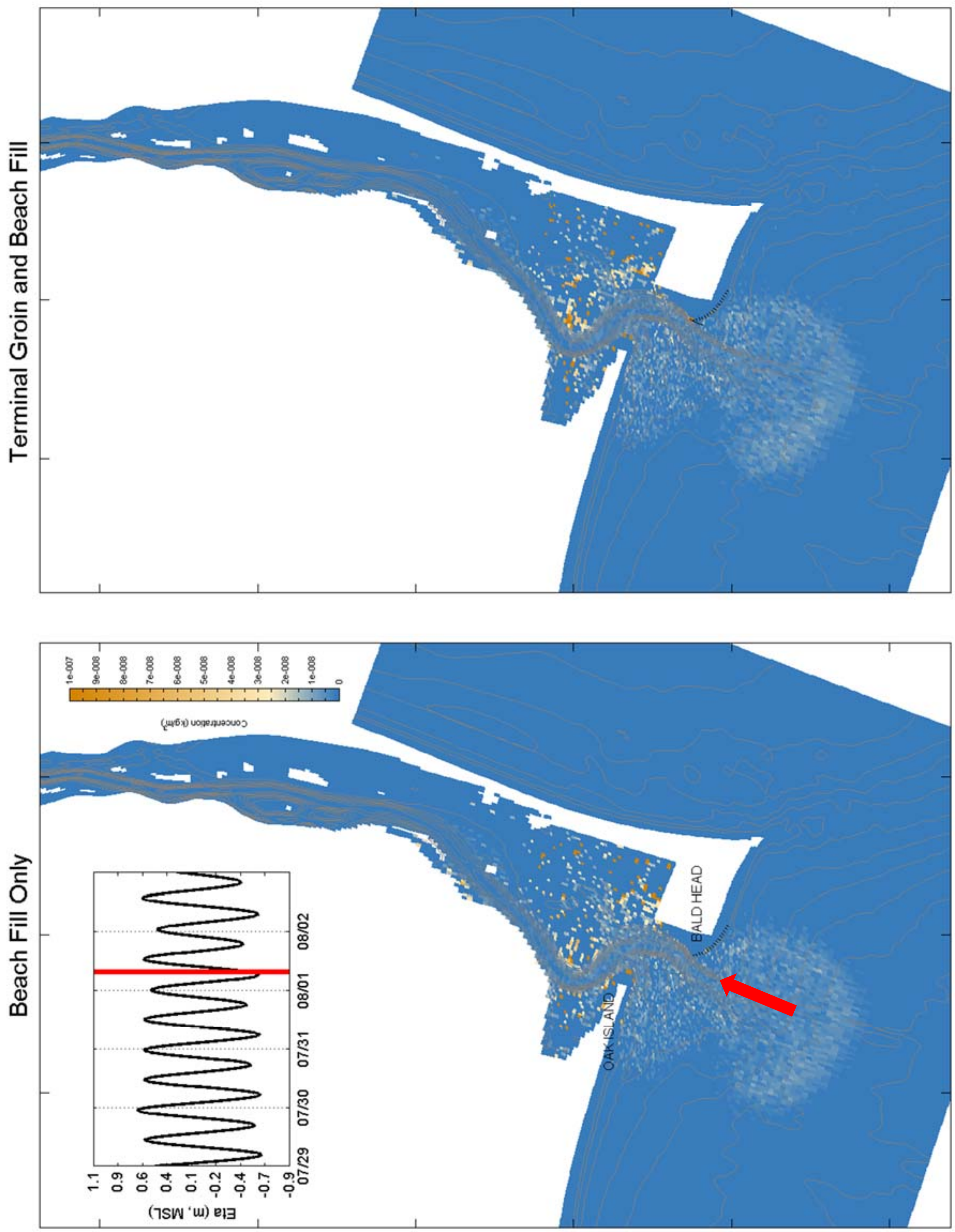

Figure 31: Particle concentration map 3.25 days following neap tide insertion.

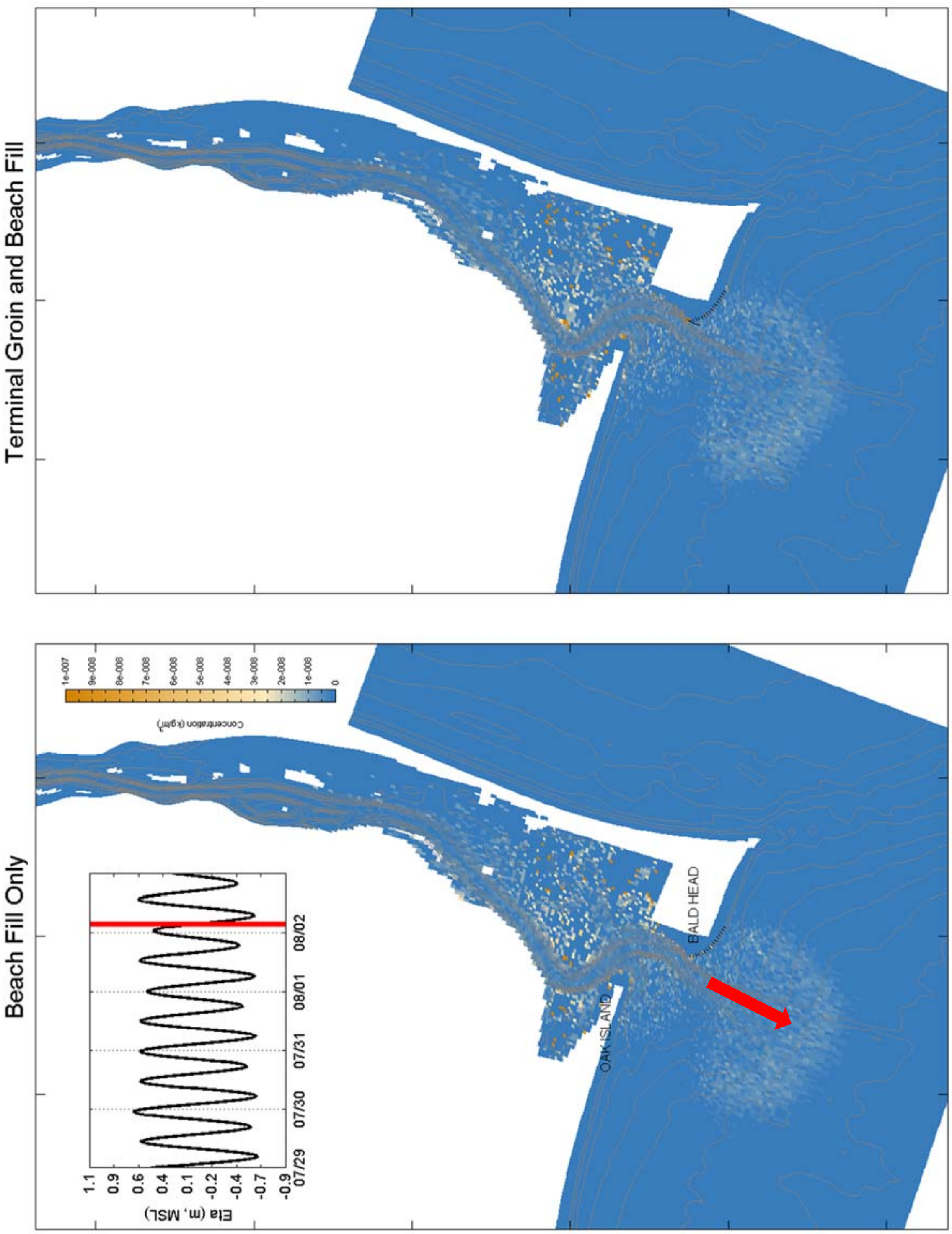

Figure 32: Particle concentration map about 4 days following neap tide insertion.

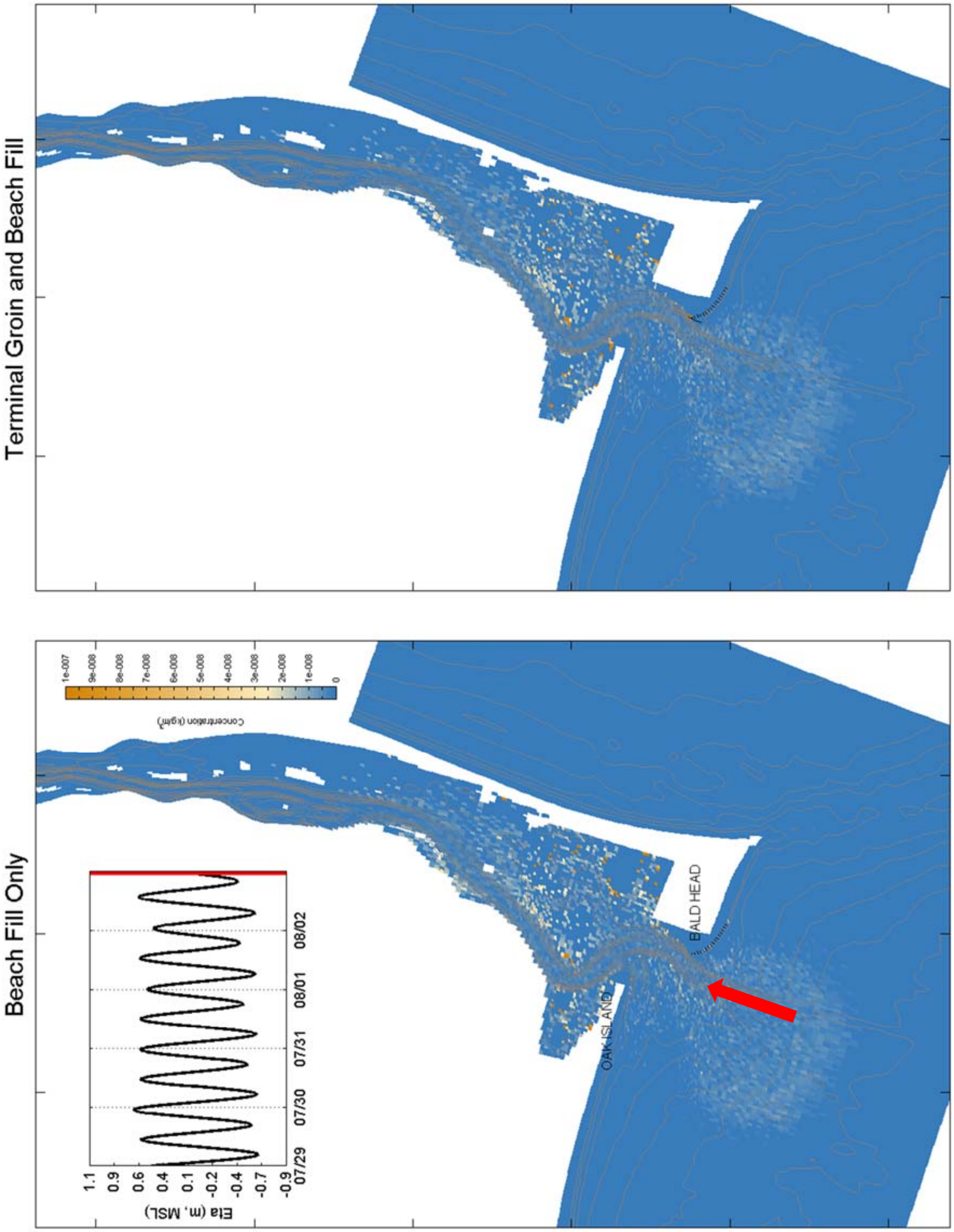

Figure 33: Particle concentration map 5 days following neap tide insertion.

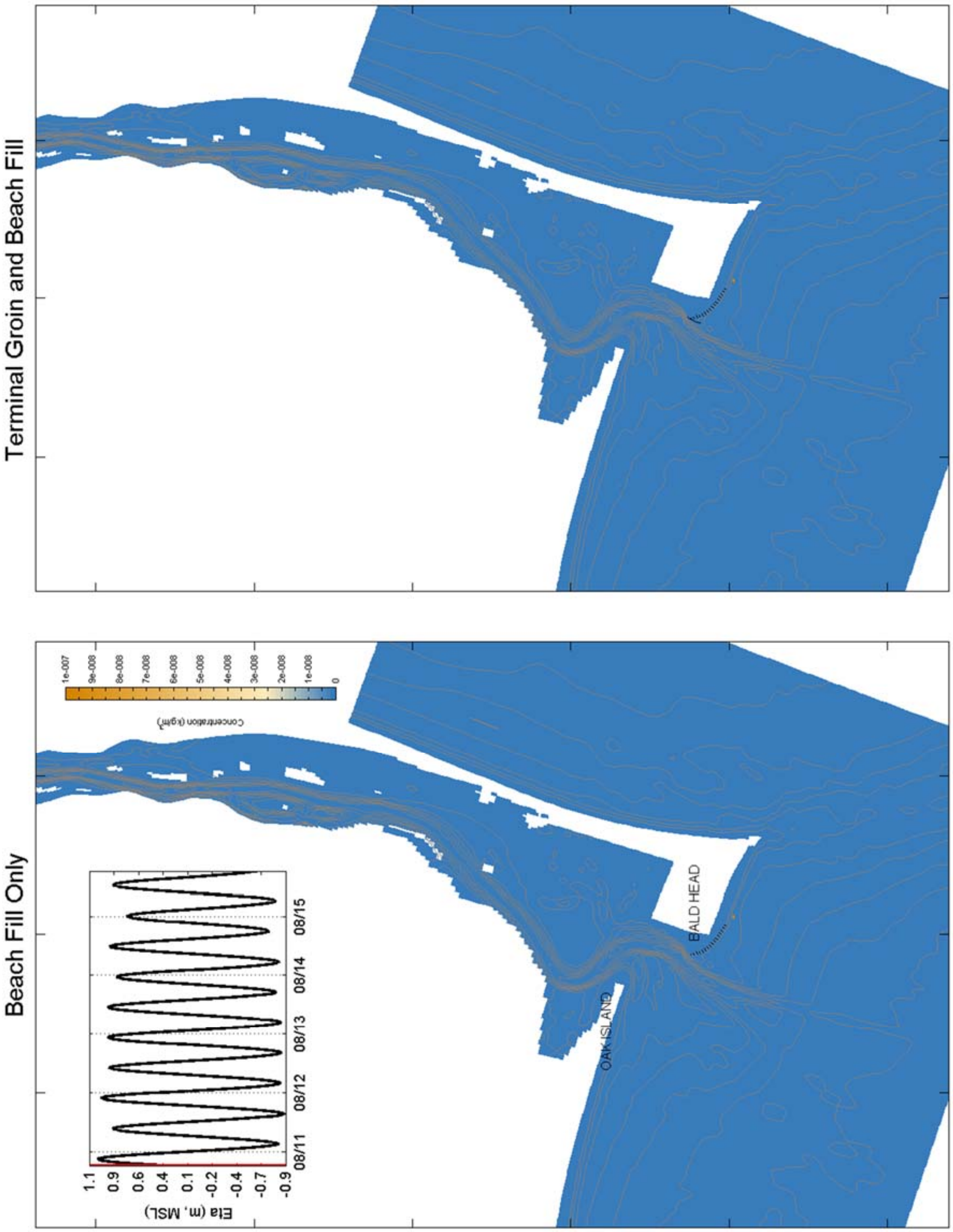

Figure 34: Particle concentration map 0 days following spring tide insertion.

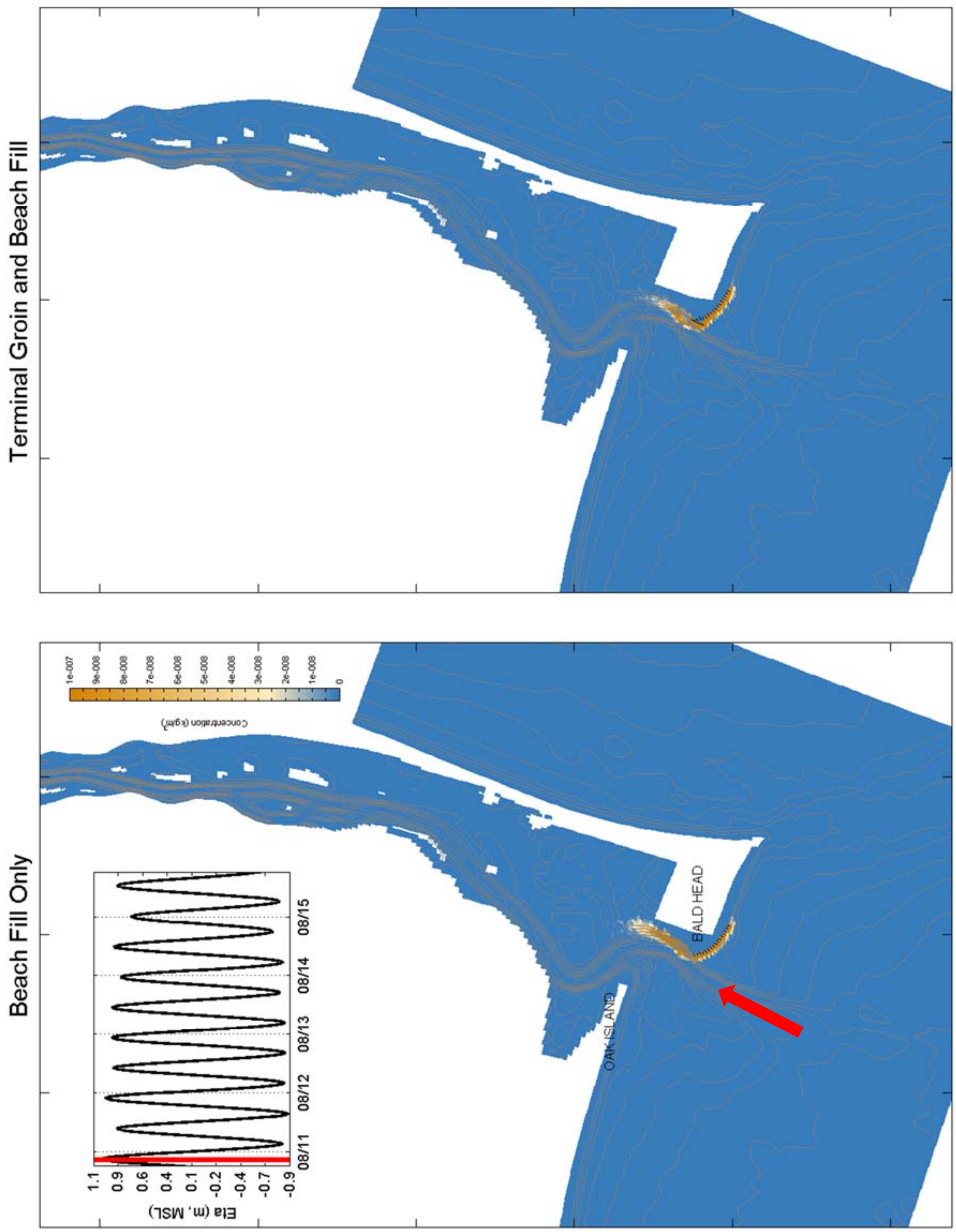

Figure 35: Particle concentration map hours following spring tide insertion.

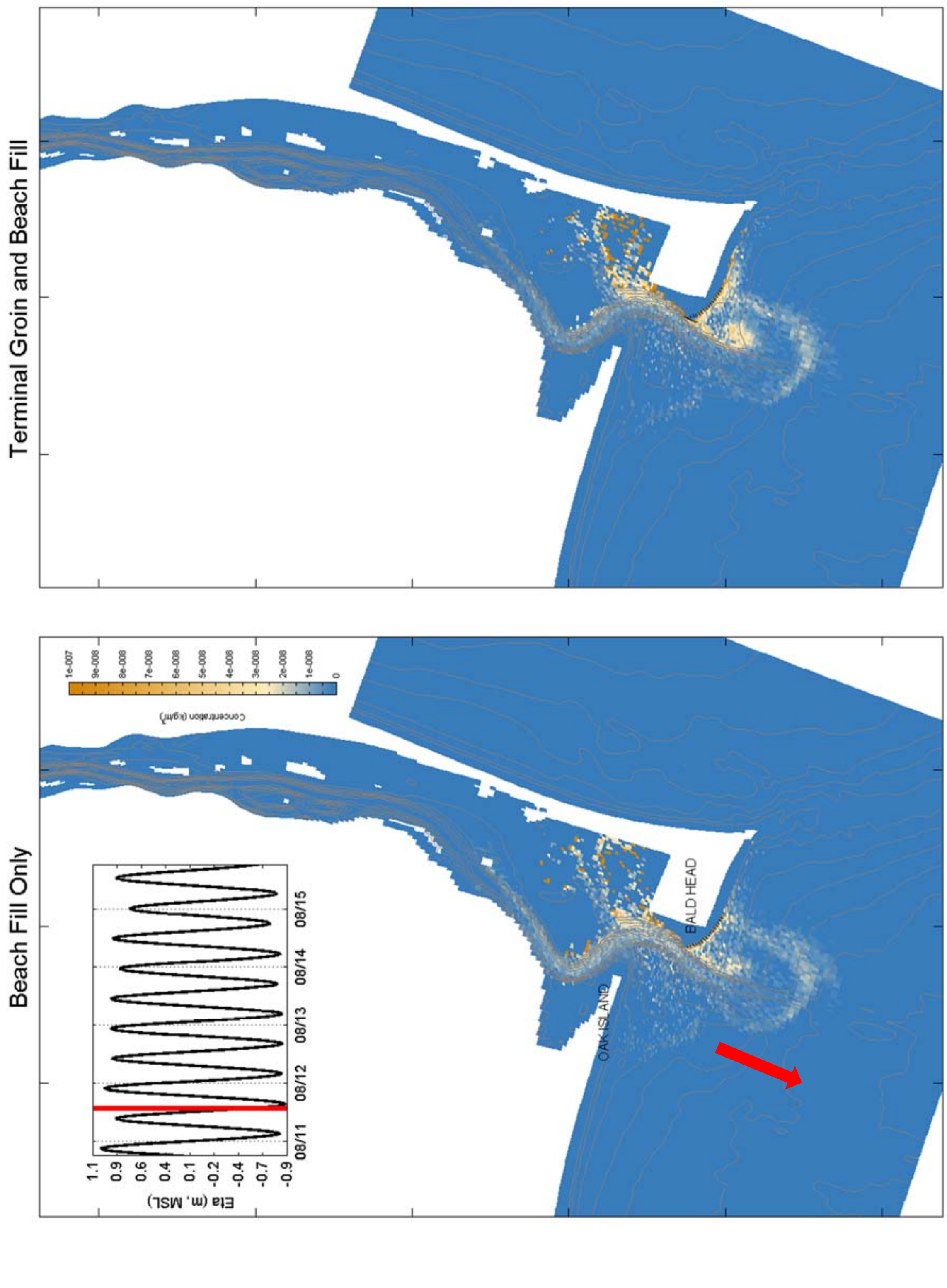

Figure 36: Particle concentration map about 1 day following spring tide insertion.

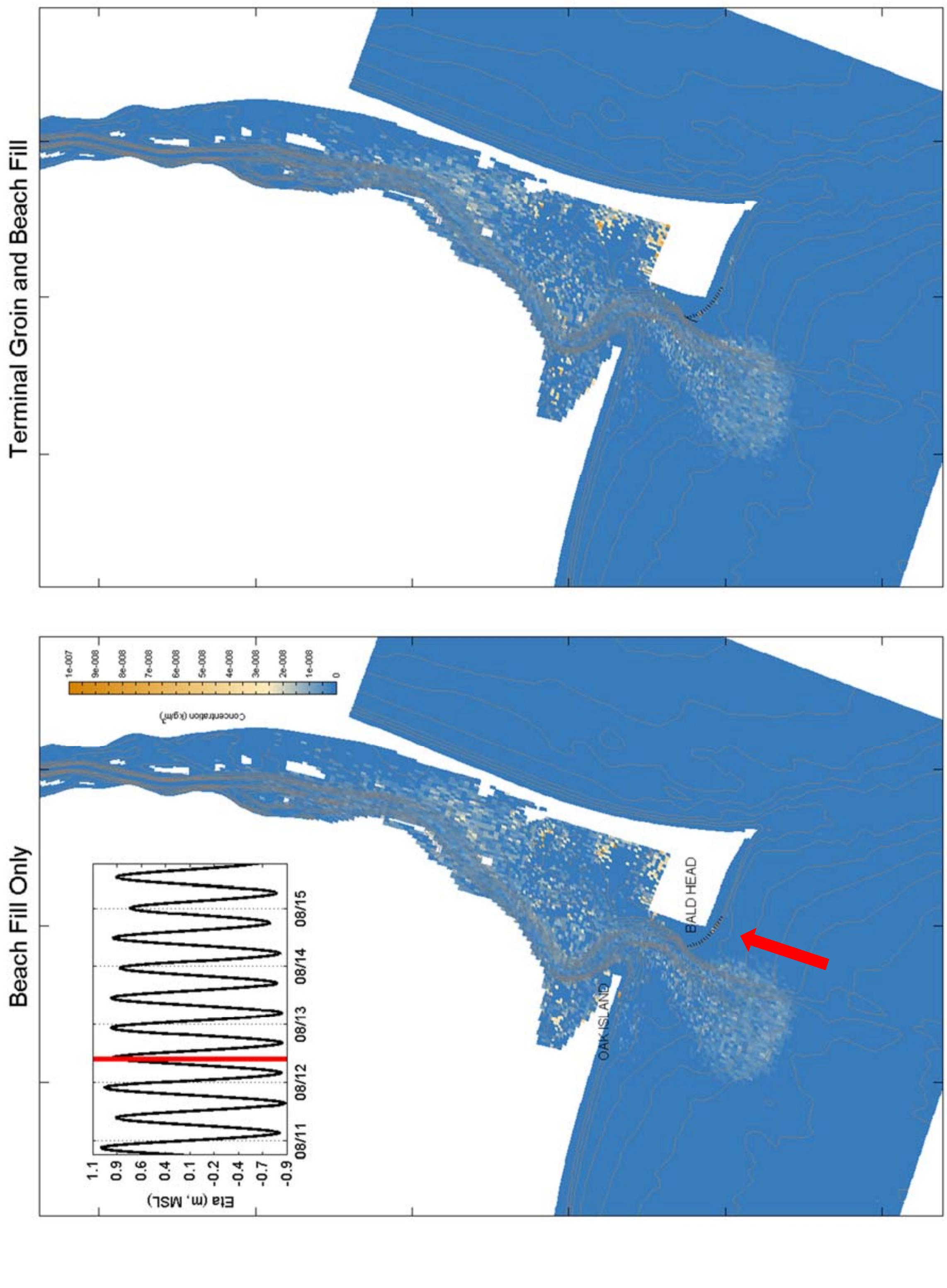

Figure 37: Particle concentration map about 1.7 days following spring tide insertion.

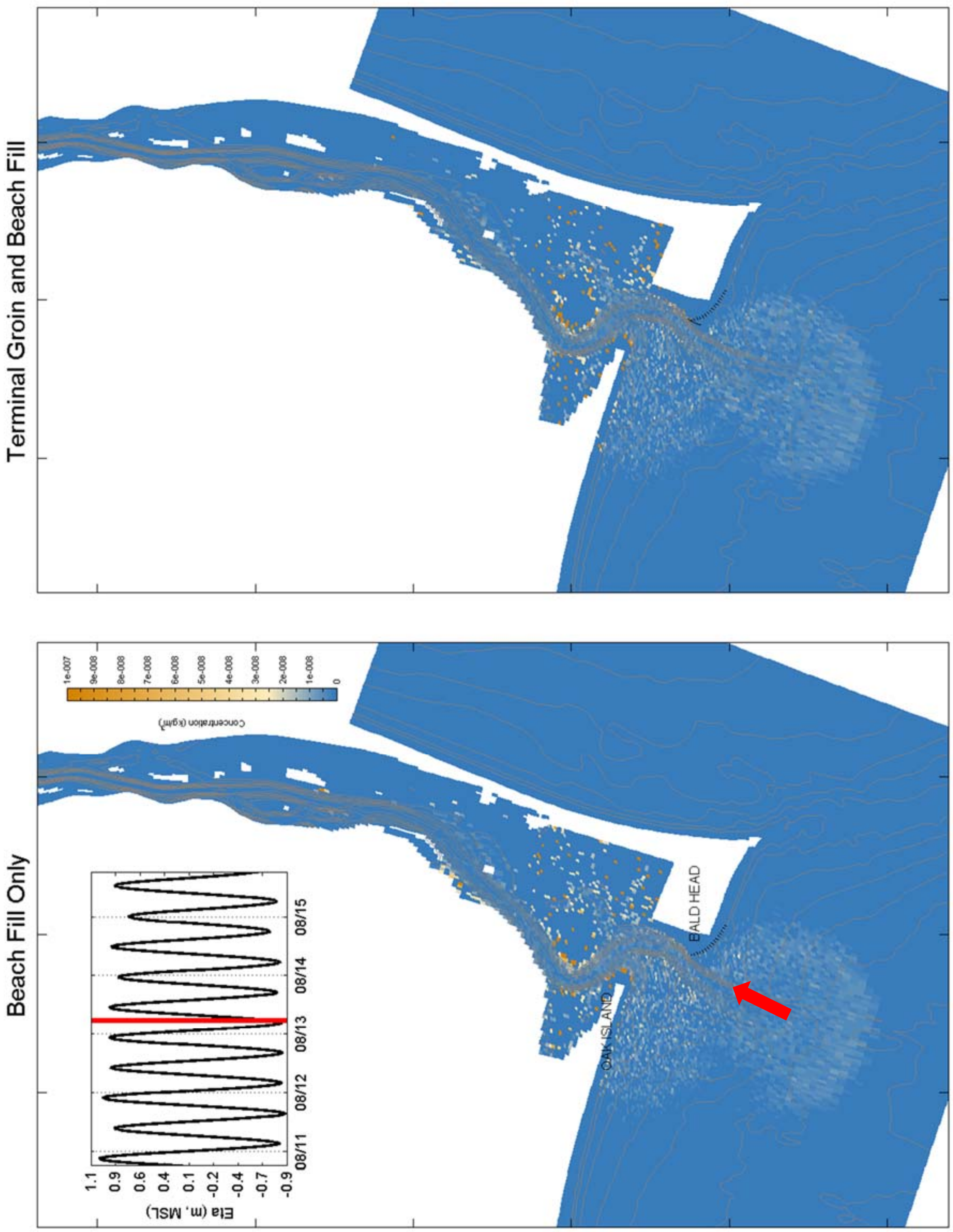

Figure 38: Particle concentration map about 2.5 days following spring tide insertion.

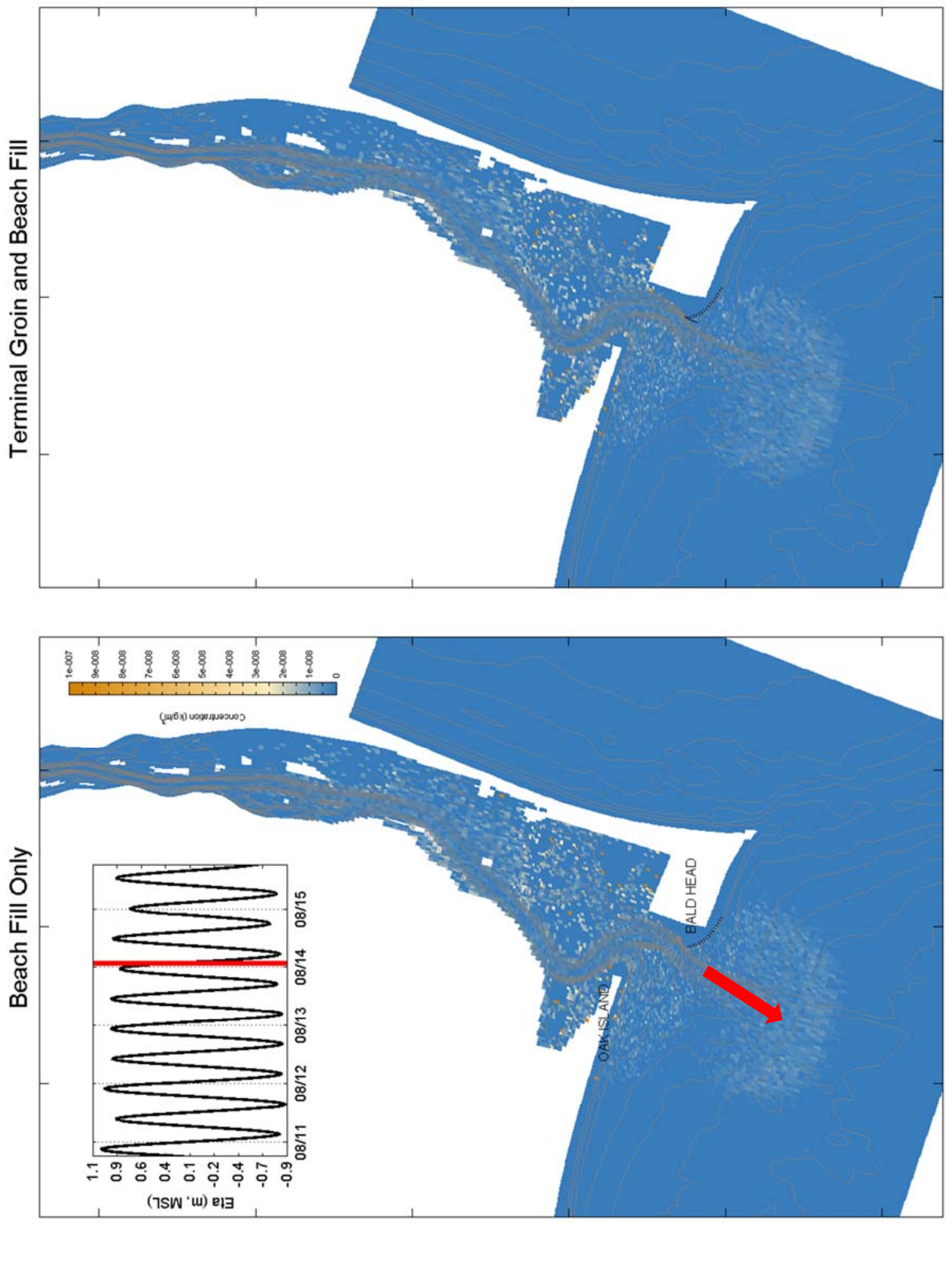

Figure 39: Particle concentration map about 3.25 days following spring tide insertion.

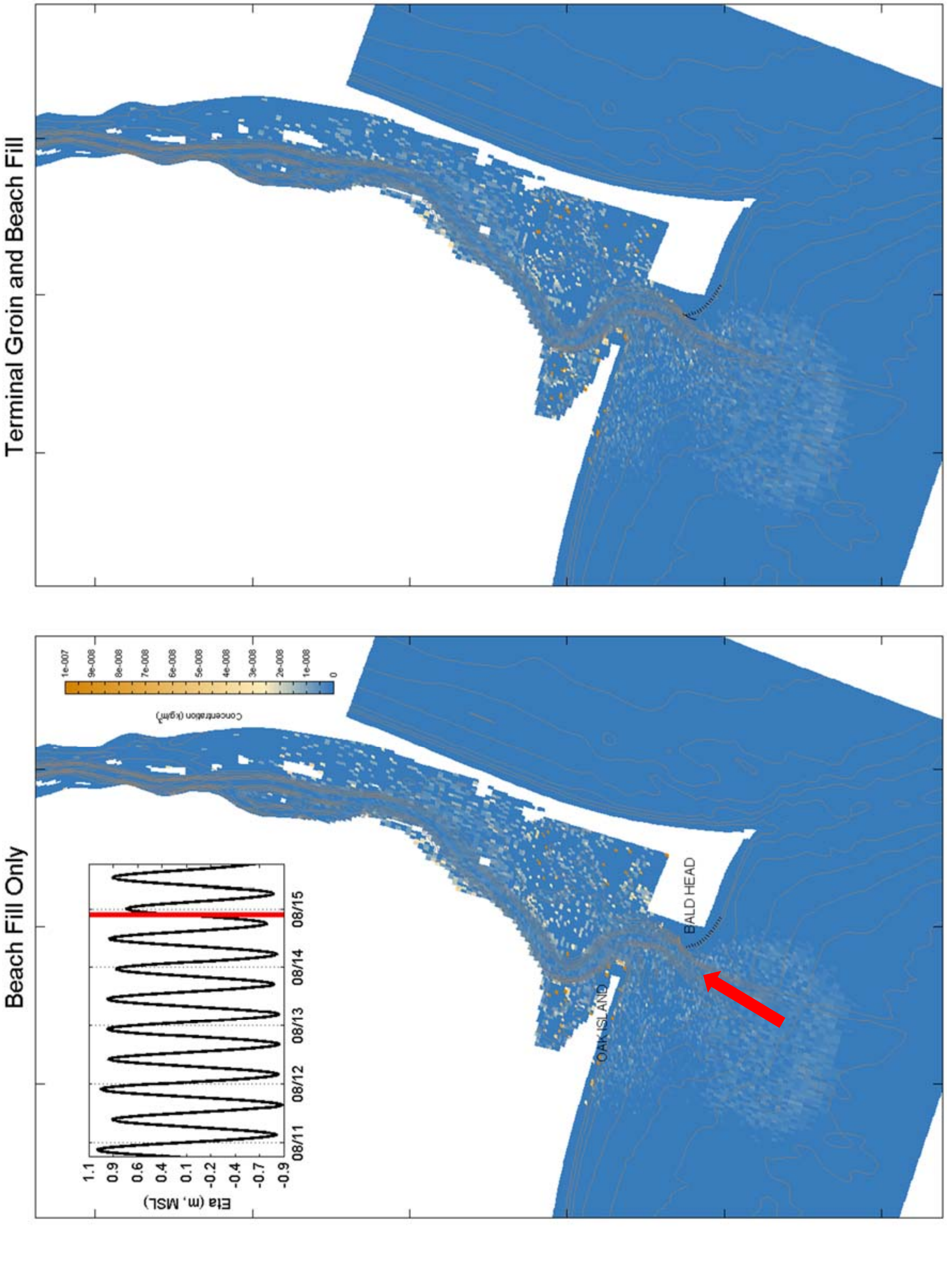

Figure 40: Particle concentration map about 4 days following spring tide insertion.

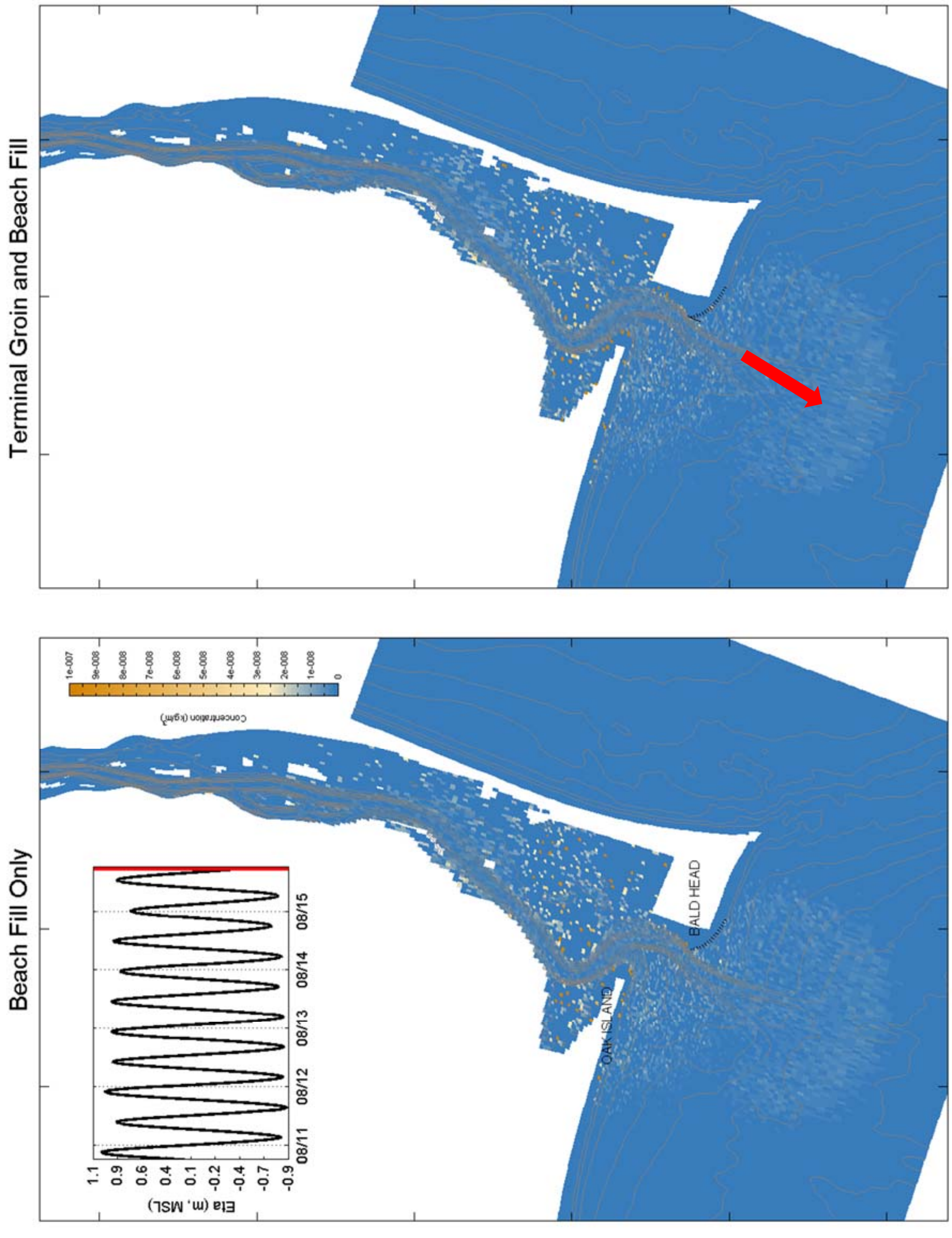

Figure 41: Particle concentration map 5 days following spring tide insertion.